EBONE

European Biodiversity Observation Network:

Design of a plan for an integrated biodiversity observing system in space and time

D5.2: Report on the use of phenology related measures and indicators for selected sites at varying spatial scales

Nicola Clerici, Christof J. Weissteiner (EC JRC)
Andrej Halabuk (ILESAS)

Final Deliverable report (Task 5.1.6; Task 5.2.1)

Ver 2.0
Document date: 09-06-2011
Document Ref.: 110516_EBONE_Final

Investigation of phenology information for forest classification using SPOT VGT and MODIS NDVI data

Nicola Clerici, Christof J. Weissteiner
EC JRC

Contents

Summary

The main goal of the present work within the context of the EBONE objectives is to investigate if leaf phenology indicators as derived from SPOT and MODIS NDVI time series can provide useful information for the detection and mapping of forest habitats, with special reference to the General Habitat Category scheme.

The report is divided into three main parts. The first one focuses on a description of the Phenolo model. This includes the pre-processing and processing steps applied to extract leaf phenology indicators from SPOT and MODIS data, and an analysis of the spatial distribution of a selection of phenometrics in test areas. The second part introduces two pilot habitat classification tests using the Random Forests™ approach and SPOT NDVI data. The last part focuses on investigating the intercalibration of GHCs with MODIS-derived phenometrics. Random Forests classifications were tested in a variety of configurations and accuracy checked using the JRC Forest Map 2006.

A set of 31leaf phenology indicators (phenometrics) was extracted using JRC Phenolo model from a time series of NDVI 10 day Maximum Value composites of 6 years (MODIS) and 11 years (SPOT).The Phenolo model considers an annual cycle of vegetation leaf phenology as represented by one permanent component, or 'background' and a variable component, function of seasonal dynamics. Pre-processing involved substitution of no data, outlier analysis and filtering. NDVI time series processing involved the extraction of date and productivity phenometrics. The model, coded in IDL, provided fast calculations in a stable environment.

The performance of the Random Forests classifications and the contribution of individual phenometrics was tested through the calculation of the Mean Decrease Accuracy parameter (MDA). Overall, the results suggest date phenometrics to be more important for forest habitat classification than productivity phenometrics, especially indicators defined around the Peak of Season point and the NDVI curve minima. Apart from areas with spatially and spectrally homogeneous forest habitat classes (Coniferous forests in Austria), the overall classification accuracy achieved with the Random Forests approach using MODIS-based phenology indicators is generally not satisfactory. We identified three main factors influencing these result: the spatial/spectral heterogeneity present in the GHC forest polygons and subsequently in the training pixels associated to these classes; the low number of training pixels available; and the use of an independent datasets to calculate accuracy which is built uniquely on spectral information. The introduction of artificial data gaps within the MODIS NDVI time series did not influence significantly classification accuracy.

On the basis of the investigation results, the following remarks were made: 1) The spatial scale of current EO-based phenology data (250 m) is at the edge of an adequate resolution for effective habitat classification with respect to GHC categories and field data; 2)It is recommended to build a large dataset of GHC training pixels in order to take into account the high spectral variability present within single GHC classes; 3) Adequate classification accuracy assessment should be based on a reference dataset not processed uniquely on spectral information, but built taking into account as much as possible the elements of heterogeneity typical of the GHCs.

The structural (height) characteristics of the life forms types considered in the General Habitat Category scheme are very valuable information which should be taken into account when using EO-derived information. For this reason, for the purpose of GHCs classification a strategy that integrates EO-based phenology indicators with EO derived information on vegetation structure from e.g. LiDAR or high resolution radar could potentially be more effective than only a phenology-based approach.

1. Introduction

The following investigation is part of the research activities of the European Biodiversity Observation NEtwork project (EBONE). The Project's main aim is to establish a framework for an integrated biodiversity monitoring and research system based on key biodiversity indicators, and implemented at institutional European level. EBONE will:

- Design a biodiversity observation network based on current national capabilities;
- Develop techniques for upscaling between sites, habitats and remote sensing data to detect and understand changes in indicators and ecosystems;
- Recommend refinements to current observation systems, and for the implementation of the proposed system in Europe;
- Integrate measurements and data structures within existing data management systems;
- Develop and test the worldwide compatibility of the system in regions outside Europe.

The EBONE project is implementing a habitat classification scheme based on *General Habitat Categories*–GHCs (Bunce et al. 2010). The main goal of the present investigation in the context of the EBONE objectives is to investigate if phenology information (phenology indicators) as derived from NDVI time series can provide valuable information for the identification and mapping of *forest* habitats as defined in the GHCs scheme (Intercalibration of EO phenology data with GHC forest phanerophytes).

More detailed objectives are:

- Derive phenology indicators of forest vegetation for the whole continental Europe at two different scales based on SPOT and MODIS data (1 km and 250 m).
- Investigate advantages and limitations of phenology based indicators for GHCs Phanerophytes (Forests) classification.
- Assess the influence of data gaps in phenology time series in GHC forest classification.

The first part of the report describes the extraction of phenology indicators (Phenolo model) for Europe. The second part describes pilot analyses using SPOT NDVI (1km) time series, showing applications of the methodology in Austria and Slovakia using Natura2000 forest habitat data and AFOLU Trees distribution data (Koeble and Seufert, 2001). A parameter measuring the performance of the classifier (OOB error) is provided, however the lack of validation data resulted in a limited assessment of classification accuracy. The last section focusses on the use of MODIS NDVI (250 m) time series for GHC forest Phanerophytes

classification. The analyses are conducted in Austria and in the MDN Environmental Zone (Metzger et al.,2005). A systematic accuracy assessment is performed.

2. Remote Sensing Data

The investigation focused on NDVI time series from the SPOT VGT and MODIS sensors, provided by the MARS Unit of the IPSC institute (EC JRC).Spatial resolution is 1km for SPOT VGT data and 250 meters for MODIS. The time series is composed of 10-days Maximum Value Composites (MVC) of NDVI, covering the following temporal windows:

- SPOT VGT: from 1999 to 2009 (11 full years);
- MODIS: from 2004 to 2009 (6 full years).

NDVI data was prepared for EC JRC by the Flemish Institute for Technological Research (VITO NV) and includes atmospheric correction, cloud detection, and calibration (Rahman & Dedieu, 1994; Paola & Schowengerdt, 1994; Klisch et al., 2005). Both NDVI datasets cover the whole of Europe. An example of SPOT NDVI mosaic for Europe is shown in *Figure 1*. Data pre-processing and processing is fully discussed in *Section 3.2* and *Section 3.3.*

Figure 1. Example of SPOT NDVI decade data for Europe (Light green: high NDVI; dark green: low NDVI; white: water/no data). Third 10 day-period in June 2007.

3. Extraction of Phenology indicators

3.1. Background

It is a frequent assumption in phenology time series analysis to assume regular patternsthat describe the vegetation leaf seasonal cycles (Jonson & Eklundh, 2004). An annual season cycle can be described in general terms as represented by a) one component which is the permanent signal, or 'background' and b) a variable component which is function of the seasonal dynamics (e.g. Weissteiner et al., 2007). The latter is generally characterized by a growing period, during which the vegetation signal intensity increases, it reaches at a certain time a peak of maximum signal (t_{MAX}), and it decreases towards the background level (senescence period). An illustrative scheme is shown in *Figure 2.*

This behaviour is ideally reflected in the NDVI signal pattern. In the real case this pattern is influenced by a number of variables which shape and modify the NDVI signal, such as meteorological factors (snow, frosts, cloud coverage) or changes in the vegetation (*e.g.*land cover change processes, health status, drought effects, etc.).

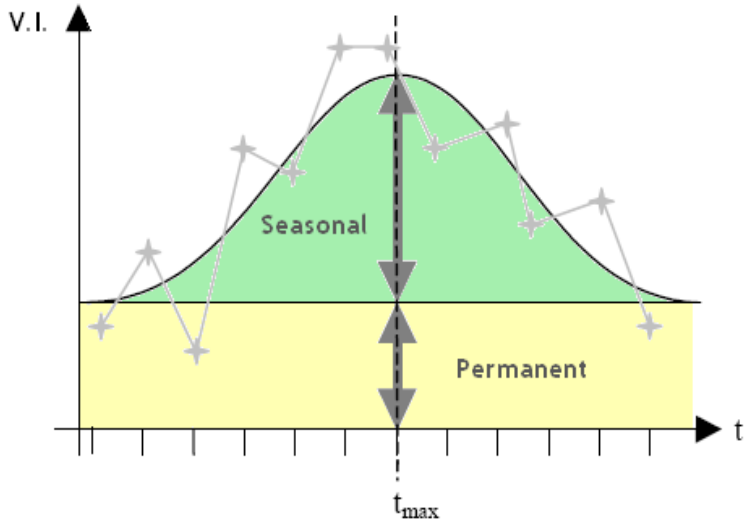

Figure 2. Observed (grey crosses) and seasonal/permanent components of a theoretical vegetation cycle (modified after Weissteiner *et al.,* 2007).

The modelling approach, developed by EC JRC (Ivits et al., 2009)on which the phenometric extraction is based, relies on the use of smoothing and moving average algorithms as a basis to extract a large set of phenology indicators. This model, called *Phenolo*, is explained in detail

in *Section 3.3*. The version of Phenolo model used in this investigation is that of 2009; a new version is currently under development.

3.2. Pre-processing

3.2.1 SPOT VGT NDVI Data

A single layer stack of SPOT NDVI data was prepared containing only those years for which full time series were available. The data series ranges from 1999-2009, comprises 396 10-days maximum value composites (hereafter called *decades*) of SPOT NDVI (built according to Holben, 1986).Missing NDVI values were already flagged as missing, clouds, snow and out rocks in the original raw data. Missing values (flagged pixels) were substituted by seasonal means when available (mean of NDVI for that decade for available years). Pixels with no seasonal mean (e.g. snow-covered throughout the same time periods of each year) were flagged. Outliers detected according to Chebychev's theorem (95 % confidence interval) were substituted by seasonal means (Lohninger, 1999). Remaining missing data were given a linear interpolated NDVI value using the nearest existing data points in time. NDVI data were filtered using a Savitzky-Golay filter (Chen *et al*. 2004), temporal window size 6x6 decades, see *Figure 3*. Finally, an aggregated mask was created adding up all single decadal masks (36) for which no seasonal mean could be calculated, combined with a water mask (*Figure 4*).

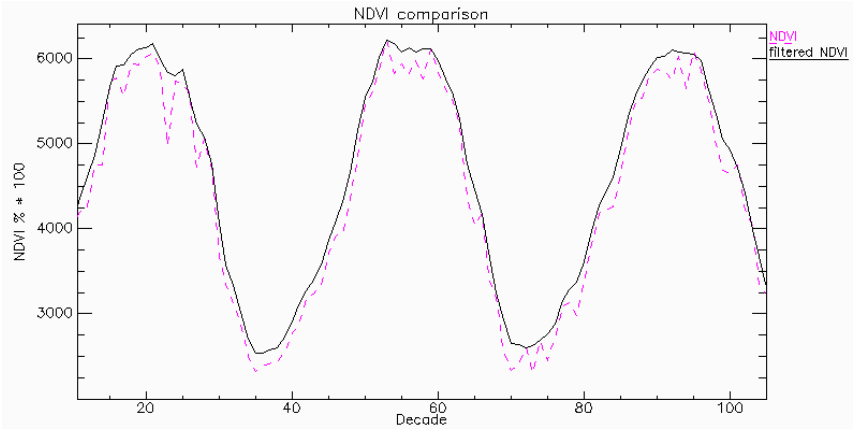

Figure 3. Example of NDVI time series before and after filtering operations with a Savitzky-Golay filter(SPOT VGT data).

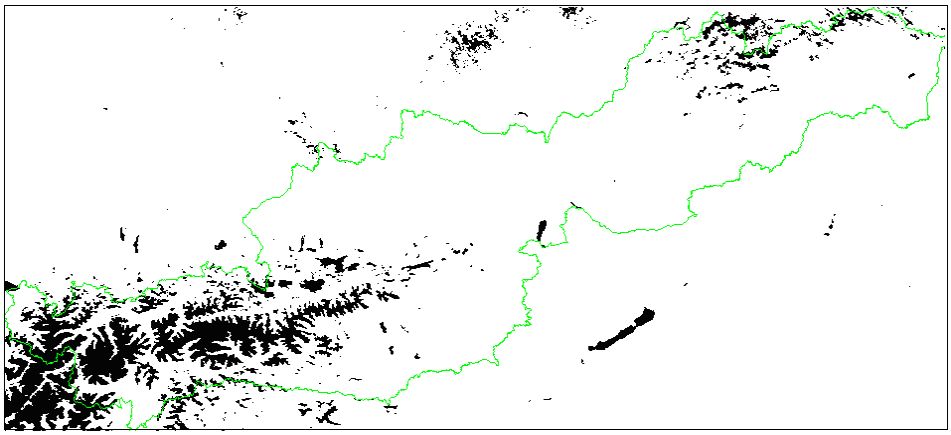

Figure 4. No data and water mask(black)for Austria and Slovakia test areas(SPOT VGT data).

3.2.2 MODIS NDVI Data

Also for MODIS NDVI data a single layer stack was prepared comprising 6 years with full data availability. For 2004-2009, the time series contained 216 10-days Maximum Value Composites (MVC) of MODIS NDVI. Missing values and outliers were substituted by seasonal means, applying the same criteria as for SPOT data. The remaining missing data were given an interpolated value between the nearest existing data points in time. Also in this case the data were filtered using a Savitzky-Golay filter (Chen *et al*. 2004) using the same specifications described in *Section 3.2.1*, and an aggregated mask was created synthesizing all single decadal masks (36) for which no seasonal mean could be calculated. A 'No data' flag layer was also derived by counting the number of decadal data gaps that are interpolated (see *Figure 26*). The following chart resumes the whole pre-processing chains.

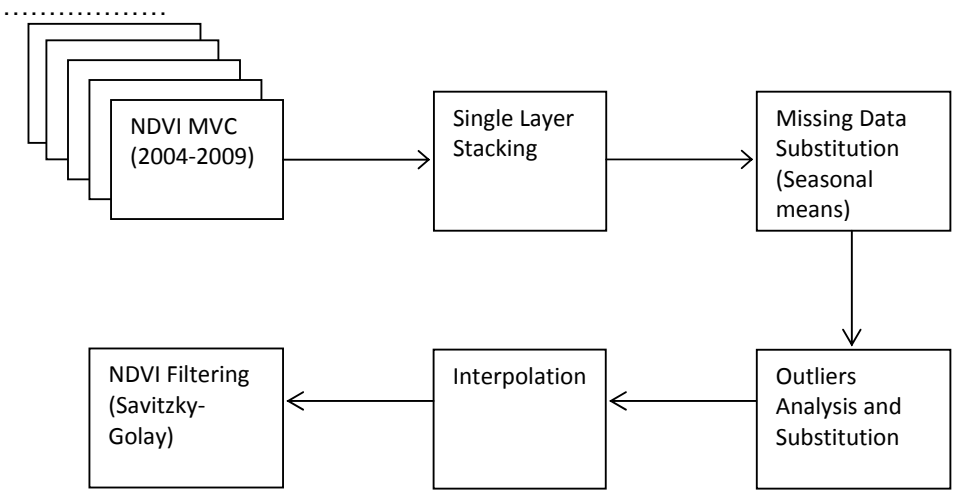

Figure 5. Pre-processing chain applied to SPOT NDVI and MODIS NDVI data.

3.3. The Phenolo model

The purpose of the Phenolo model, developed by EC JRC (Ivits et al.,2009), is to extractleaf phenological indicators from time series of vegetation indices. In the first step the model appliesa median filter on a sliding temporal window of 5 successive time points. This is followed by the calculation of one forward and one backward lagging curve using a moving average algorithmFor example, for a forward lag, an *x*-day moving average value of time point *p* is calculated as the average of values for the *x* time points from *(p-x)* to *p*. The resulting averaged values will always reach similar magnitudes as the original p values later in time. The lag distance (defined in terms of the number of successive time points *x*) is defined by applying 1 standard deviation from the barycentre of the integral surface of the curve (*Figure 6*, Ivits et al., 2008). This value can be changed according to analysis needs.

Phenology Indicators

A number of studies investigated vegetation dynamics using information from date phenometrics (e.g. Reed et al., 1994; Hill and Donald, 2003); all of them considered a start and end of growing season. Following Reed et al. (1994), the start of the growing season (SOS in *Figure 6*) is defined as the crossing point between the smoothed curve and the forward lagged curve. The same criterion applies for the end of season (EOS), defined as the intersection between the backward curve and the smoothed one.The point corresponding to the maximum value of the vegetation signal is the Peak of Season (POS in *Figure 6*). The Growing Season End (GE) is defined as the point when, following the EOS, the forward lagged curve that defines SOS intersects the signal curve. The EOS, SOS, POS and GE points define two phenology indicators each: the correspondent day and NDVI value (see Table 1). The time interval in days between SOS and EOS defines the Season Length (SL), while the time interval between the minima in the phenology curve is referred in the model as Total Length (TL). For further details on the phenology indicators construction see Ivits et al. (2008, 2009).

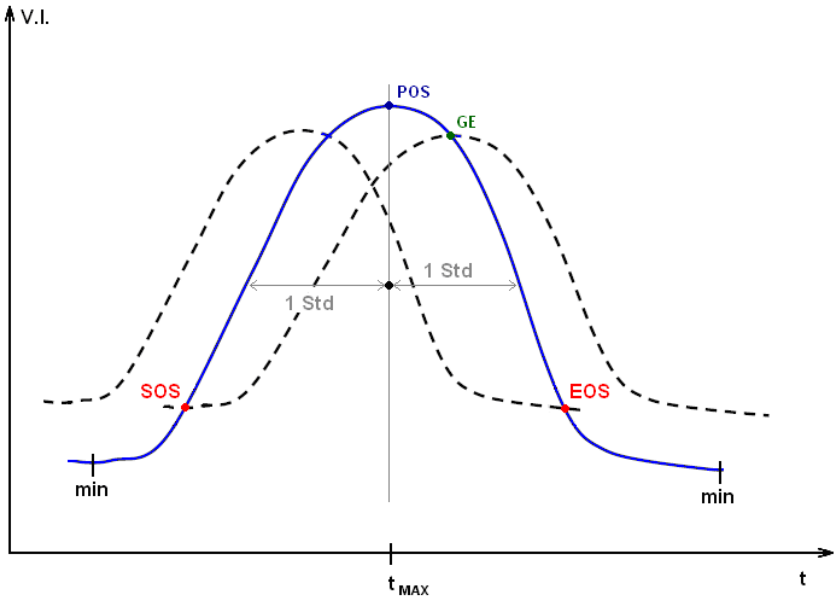

Figure 6. Smoothed curve (blue) and forward and backward lagging curves (dotted) defining date phenometrics in Phenolo (after Ivits et al., 2008).

From the phenology curve it is also possible to define a series of *productivity* phenometrics (e.g. in *Figure 7*), a selection of which are:

- *Seasonal Permanent Fraction* (SPF), defined by the area between the line connecting Start and End of season and the x axis;
- *Season Integral* (SI), is the integral under the vegetation signal curve delimited by the start and the end of season;
- *Total Permanent Fraction* (TPF), is the area between the timeline connecting the vegetation signal minima and the x axis;
- *Total Integral* (TI), is the integral under the vegetation signal curve delimited by the two vegetation signal minima. TI is a proxy that represents an approximation of the Net Primary Productivity.

The GE point defines the Growing season Integral (GI) and derived integrals (see *Table 1*). Other phenology indicators, derived mathematically from the phenometrics listed above, are also extracted by Phenolo (see *Table 1*, indicators list and short explanation).

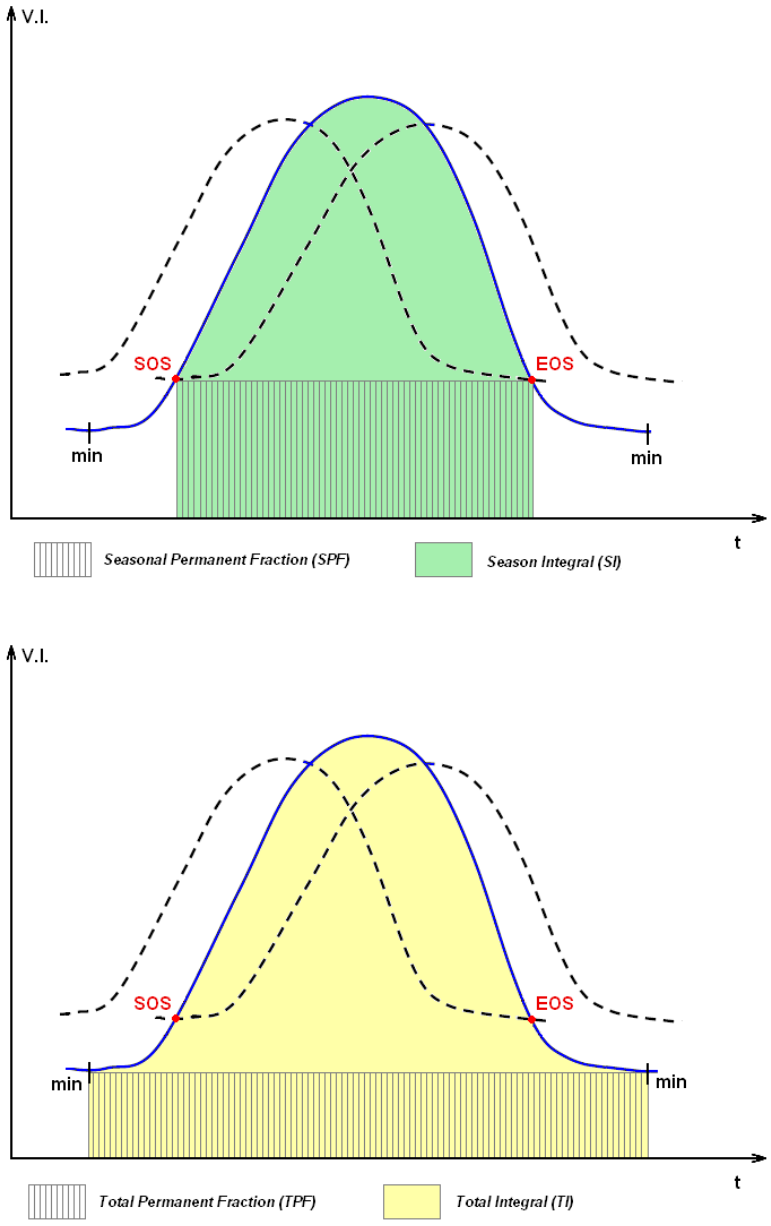

Figure 7. A selection of productivity phenometrics extracted by Phenolo (modified, after Ivits et al., 2009).

Table 1. Phenometrics extracted by Phenolo, with short explanation and acronyms defined in the Phenolo model. (*GTR was finally discarded).

Acronym used in text	***Phenometric extracted and short explanation***	*Acronym in Phenolo*
SOS	Start of season (Day)	*SBD*
"	Start of season (Value)	*SBV*
EOS	End of season (Day)	*SED*
"	End of season (Value)	*SEV*
SL	Length of Season (EOS-SOS)	*SL*
SI	Season Integral: the integral under the vegetation signal curve delimited by EOS and SOS	*SI*
SNI	Normalized SI	*SNI*
SPF	Seasonal Permanent Fraction: the area below the line connecting SOS with EOS, and the *x* axis.	*SPI*
STR	Season Total Ratio [SI/(SI+SPF)]	*STR*
GE	Growing Season End (day)	*GED*
GE	Growing Season End (value)	*GEV*
GL	Growing Season Length	*GL*
GI	Growing Season Integral	*GI*
GNI	Normalized GI	*GNI*
GTR*	Growing Season Total ratio [GI/(GI+SPF)]	*GTR*
GPI	Growing Season Permanent Fraction: the permanent area fraction below the curve connecting SOS with End of growing season	*GPI*
MBD	Minimum before SOS (Day)	*MBD*
MBV	Minimum before SOS (Value)	*MBV*
MED	Minimum after EOS (Day)	*MED*
MEV	Minimum after EOS (Value)	*MEV*
TL	Total Length: Length in time between minima (Days)	*ML*
TI	Total Integral: the area under the vegetation signal curve delimited by the two minima.	*MI*
NTI	Normalized TI	*MNI*
MTR	Above Minima Total Ratio: above minima integral over TI	*MTR*
TPF	Total Permanent Fraction: the area below the line connecting the vegetation signal minima and the x axis.	*MPI*
SEI	Season Exceeding Integral: (TI-SI)	*SEI*
GEI	Growing Season Exceeding Integral: (TI-GI)	*GEI*
SBC	Season Barycentre	*SBC*
SSD	Standard Deviation of the Season vegetation curve	*SSD*
POS	Peak of Season (Day)	*MXD*
"	Peak of Season (Value)	*MXV*
OMI	Output minus Input Length (365 – GL)	*OMI*

4. Analyses

4.1. Exploring the use of NDVI derived phenometrics using SPOT Data

4.1.1 Introduction

Extraction of phenometrics was performed for both SPOT and MODIS NDVI time series. Initial (pilot) tests were carried out using SPOT NDVI data, as the processing of SPOT data is less computationally intense. Austria and Slovakia were chosen as study areas. The pilot study involved: 1) testing the feasibility of methods applied and implemented throughout the different stages from phenometrics extraction to forest habitat / species classification;2) deriving measures of reliability of the Random Forests classifier, using Natura2000 forest habitat data and AFOLU Trees distribution data (Koeble and Seufert, 2001).

The three main sequential blocks of data processing carried out were as follows:

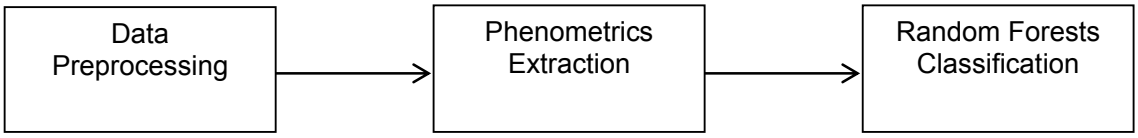

A short phenological characterization of the study area is shown using date and productivity phenometrics. A formal classification accuracy assessment was not performed for the SPOT analysis, as the main aim of this task was to test the phenology model and the Random Forests classification routines. Instead, a systematic accuracy assessment was performed in the MODIS NDVI classification in the second part of the analyses work (*Section 4.2*).

4.1.2 Phenological Characterization of test sites

To provide a general phenological characterization of the test area, the average and standard deviation of the phenometrics extracted were calculated using as spatial units the *Environmental Strata (EnS)* delineated by Metzger *et al*. (2005). In other words, the mean value of the phenometric for the NDVI time series was averaged over all locations belonging to each EnS. Metzger's bio-geographical division, together with the upper hierarchy level -*Environmental Zone*-, is considered an up to date and appropriate stratification for environmental modelling exercises and reporting in the European region. *Figure 8* shows the

Environmental Zones (EnZ) and Environmental Strata (EnS) present in the study area. The region is dominated by the Alpine South (ALS), Continental (CON) and Pannonian (PAN) EnZ with small areas representing the Mediterranean Mountains (MSM) and Alpine North (ALN) EnZ. A further sub-division in Environmental Strata is also shown. For detailed construction of EnZ and EnS see Metzger *et al*. (2005).

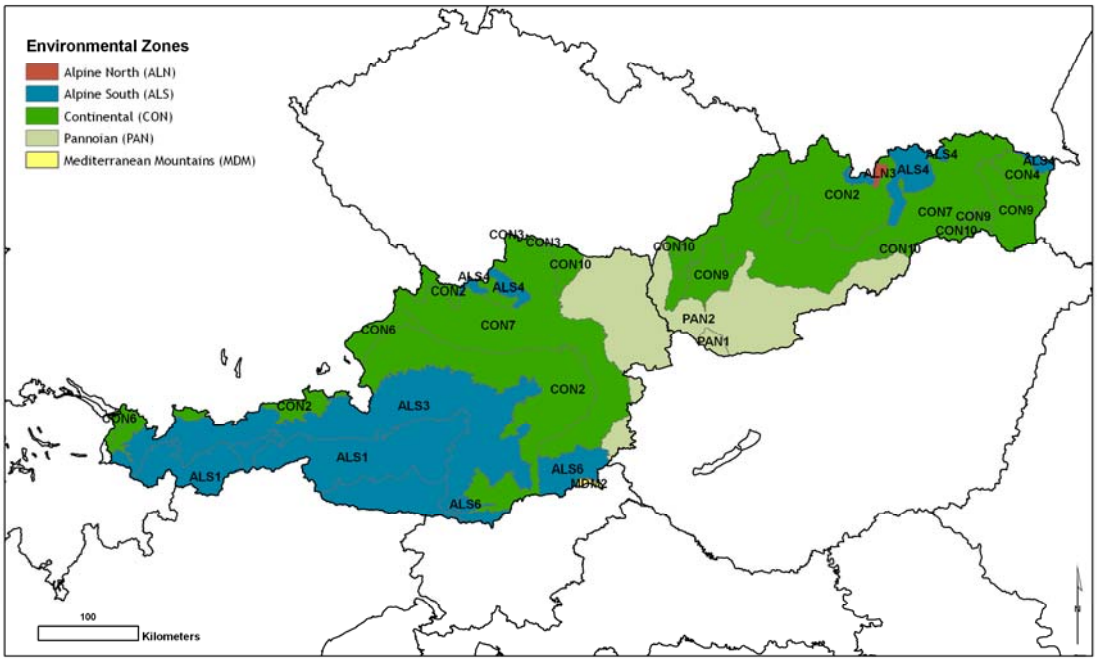

Figure 8. Environmental Stratification (EnZ, EnS) in the study area (after Metzger *et al.,* 2005).

The Corine2000 dataset (EEA, 2010) was used to mask out non-vegetated areas from the mean and standard deviation statistics. This operation eliminates all pixels representing a) water bodies, b) built areas and c) bare rocks.

To get an interpretation key regarding the distribution of phenology indices, altitude statistics from the GTOPO30 dataset and land-cover information from the GLC2000 map were extracted and summarised per EnS (*Table 5.1*, *Table 5.2*).

The following representative phenology indices were selected to illustrate their distribution throughout the study area (see *Section 3.3* for more detail on the phenology parameters):

- Seasonal Permanent Fraction (SPF);
- Total Integral (TI);
- Peak of season value (MXV).

Table 2. Altitude Statistics per Environmental Strata as derived from GTOPO30 data.

EnS	ALN3	ALS1	ALS3	ALS4	ALS5	ALS6	CON10	CON2	CON3	CON4	CON6	CON7	CON9	MDM2	PAN1	PAN2
Mean height (m)	1498	2038	1279	733	1463	376	317	817	487	386	467	470	177	231	111	192
Min height (m)	852	648	423	318	225	230	160	326	424	109	316	126	93	201	106	102
Max height (m)	2348	3713	2805	1409	3179	914	541	2031	562	965	1373	1312	537	296	124	584

Table 3. Percentage of land cover type (GLC2000) per Environmental Strata (in bold the dominant class/es in the correspondent EnS). Masked classes are not reported.

EnS	*Tree cover, broadleaved, deciduous, closed (%)*	*Tree cover, needle-leaved, evergreen (%)*	*Tree cover, mixed leaf type (%)*	*Shrub cover, closed-open, deciduous (%)*	*Herbaceous cover, closed-open (%)*	*Sparse herbaceous or sparse shrub cover (%)*	*Mosaic: Cropland / Shrub and/or grass cover (%)*	*Cultivated and managed areas (%)*
ALN3	3.44	**75.40**	0.79	0	0	19.05	0	0.79
ALS1	5.05	**30.67**	2.12	0.34	**30.87**	25.41	0	0
ALS3	14.35	**54.55**	12.31	0.44	11.00	6.47	0.01	0.40
ALS4	23.24	**43.06**	7.71	0	0.35	0	0	25.33
ALS5	15.52	**54.64**	9.08	0	12.98	6.69	0	0.41
ALS6	**64.79**	11.23	10.26	0	0.64	0	0	11.62
CON10	17.90	4.83	1.56	0	0	0	0	**74.57**
CON2	23.43	**52.57**	11.07	0	3.48	0.08	0.02	8.58
CON3	0	15.96	5.32	0	0	0	0	**78.72**
CON4	**87.22**	0.36	0.16	0	0.12	0	0	11.74
CON6	**29.23**	9.61	9.02	0	17.67	0	1.48	**28.44**
CON7	**44.50**	14.62	5.00	0	1.00	0	0	33.84
CON9	15.99	2.83	0.71	0	0.09	0	0	**78.83**
MDM2	22.97	12.92	8.61	0	0	0	0	**55.50**
PAN1	3.35	1.80	1.16	0	0	0	0	**91.51**
PAN2	11.23	3.30	0.41	0	0.23	0	0	**81.30**

Seasonal Permanent Fraction

The Seasonal Permanent Fraction (SPF) is a phenological parameter defined as the area between the line connecting Start and End of season and the x axis. It refers approximately to the part of the vegetation signal which is permanent throughout the season. The average SPF and standard deviation values calculated for the two data series are presented in *Table 5.3*.The SPF averages from SPOT and MODIS reveal consistent differences in magnitude with the SPOT derived SPFs being lower than MODIS derived SPFs (linear correlation Pearson's ρ = 0.89). In other words, the resulting spatial pattern found across the study area of the average SPF or average level of permanent greenness is similar for both data series. As an example, the contiguous Environmental Strata PAN1, PAN2, CON9 and CON10 belong to the lower SPF classes for both data series. The land cover distribution of these environmental strata show a dominance of the 'Cultivated and managed areas' which is likely to have strongly influenced the vegetation signal: The low SPF is possibly due to prolonged periods of no vegetation in the crop fields, occurring on and off throughout the year.

The SPF Standard deviations are much higher when MODIS data is used; this is possibly a consequence of MODIS pre-processing algorithms, which required the substitution of a higher number of no data than SPOT. The different number of years that characterize the SPOT and MODIS time series (11 yrs and 6 yrs respectively) is likely to produce an effect on the mean values, thus comparisons between datasets are only indicative.

The spatial distribution of the mean SPF per Environmental Strata is presented in ***Figure 9*** for SPOT and in ***Figure 10*** for MODIS data.

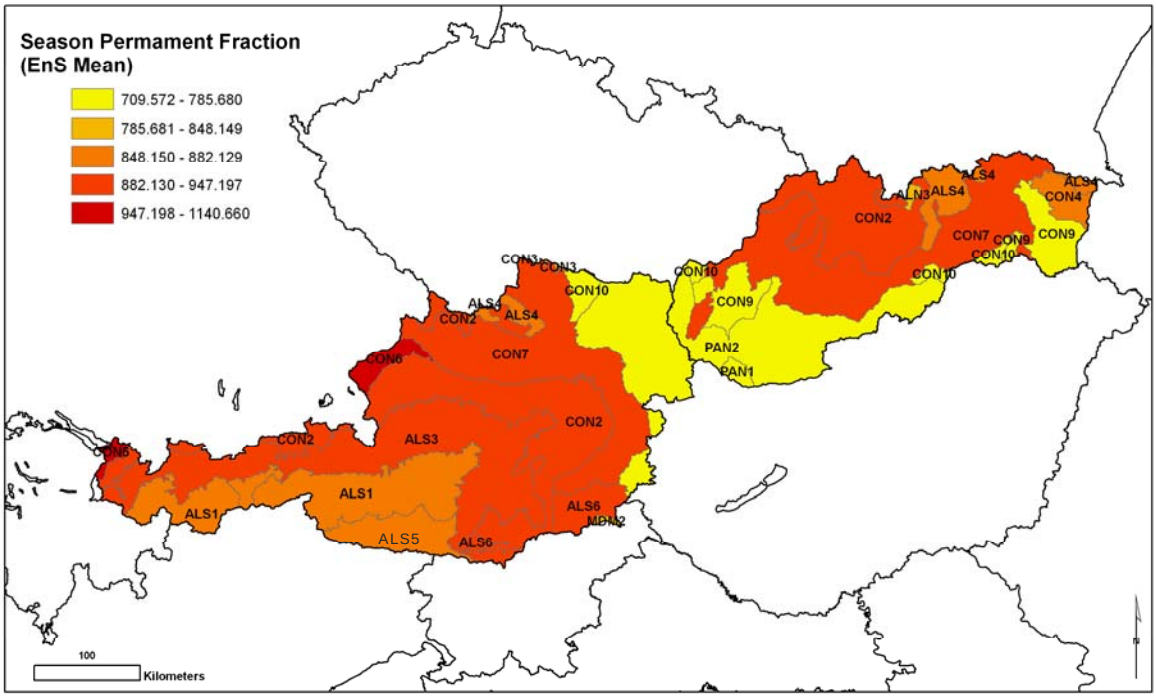

Figure 9. Distribution of Mean SPF per Environmental Strata (SPOT NDVI data).

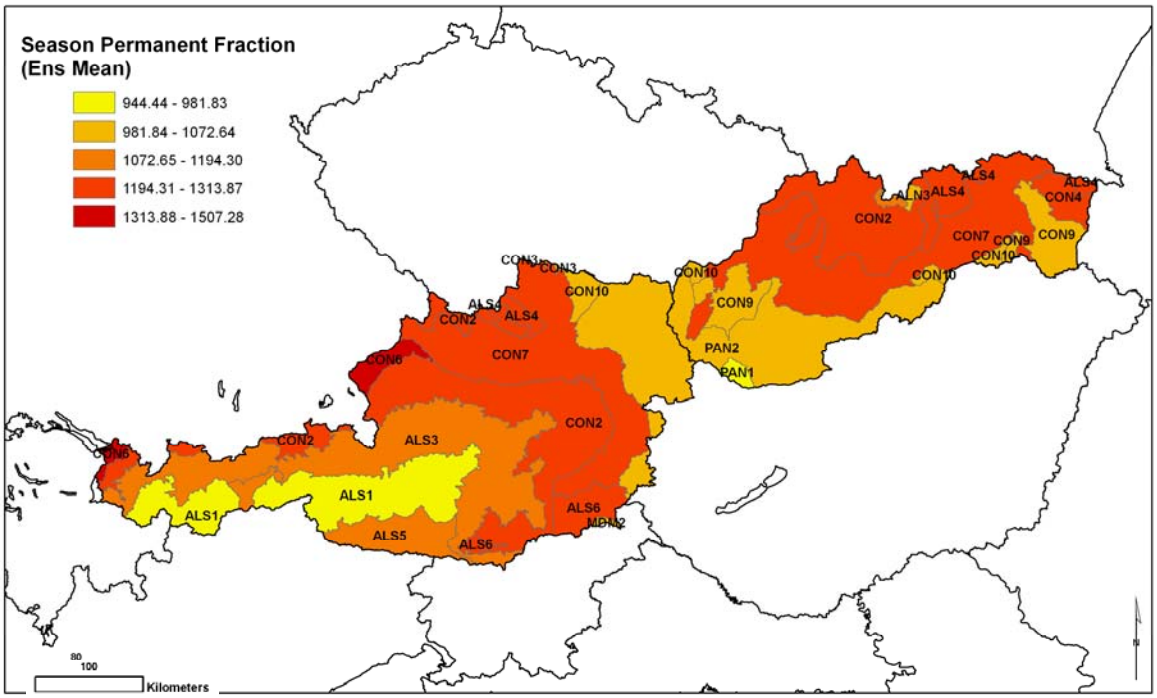

Figure 10. Distribution of Mean SPF per Environmental Strata (MODIS NDVI data).

Table 4. Mean SPF and standard deviation values per Environmental Strata (SPOT and MODIS data) and associated scatterplot (SPOT vs MODIS NDVI EnS average).

EnS	*SPOT*		*MODIS*	
	SPF mean	*SPF std*	*SPF mean*	*SPF std*
ALN3	830.67	86.22	1028.90	261.42
ALS1	856.74	95.73	944.437	288.82
ALS3	915.42	116.87	1194.30	288.84
ALS4	877.94	102.09	1239.66	180.93
ALS5	882.12	129.24	1139.58	302.48
ALS6	915.17	104.02	1262.37	216.00
CON10	785.68	80.19	1032.96	216.45
CON2	947.19	130.61	1313.87	227.49
CON3	848.14	110.85	1072.64	300.91
CON4	878.47	38.77	1252.46	91.530
CON6	1140.66	119.01	1507.28	218.05
CON7	919.61	109.30	1267.42	186.46
CON9	769.78	84.26	1040.98	197.73
MDM2	817.08	57.03	1055.76	188.80
PAN1	709.57	53.42	981.828	152.95
PAN2	772.59	92.49	1010.06	207.19

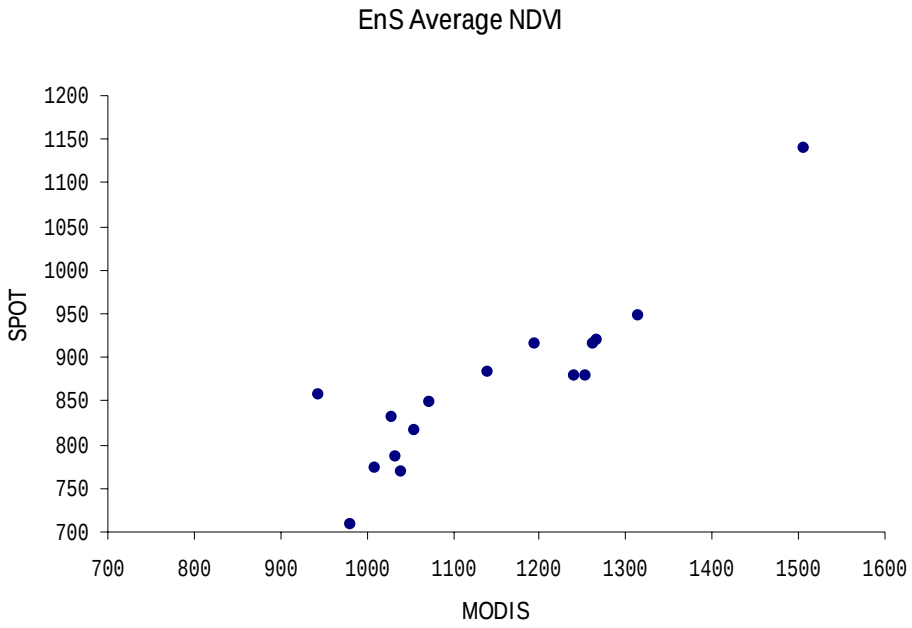

Total Integral

The Total Integral (TI) phenometric represents the area under the NDVI curve delimited by the two vegetation signal minima. TI is an important proxy representing an approximation of the Net Primary Productivity (NPP), see Reed et al. (1994). Mean TI and standard deviation values calculated for the two data series are presented in Table 5.

Again, the mean and standard deviation show differences in magnitude between the two data series with TI mean and stdev values from SPOT being consistently lower than those from MODIS. The Continental environmental strata (CON), which in the study area are characterized mainly by natural broadleaf forests (GLC2000), showed in both data series the highest values of TI. This suggests that in this study area the CON stratum is one of the more productive. Lower productivity is related to the Alpine (ALS1) and the Pannonian strata (PAN1, PAN2), characterized by lower productive vegetation, such as, respectively, natural herbaceous vegetation and cultivated fields.

The spatial distribution of mean TI is presented in *Figure 11* for SPOT data and in *Figure 12* for MODIS data. Data correlation between the two mean series is very high (ρ = 0.96).

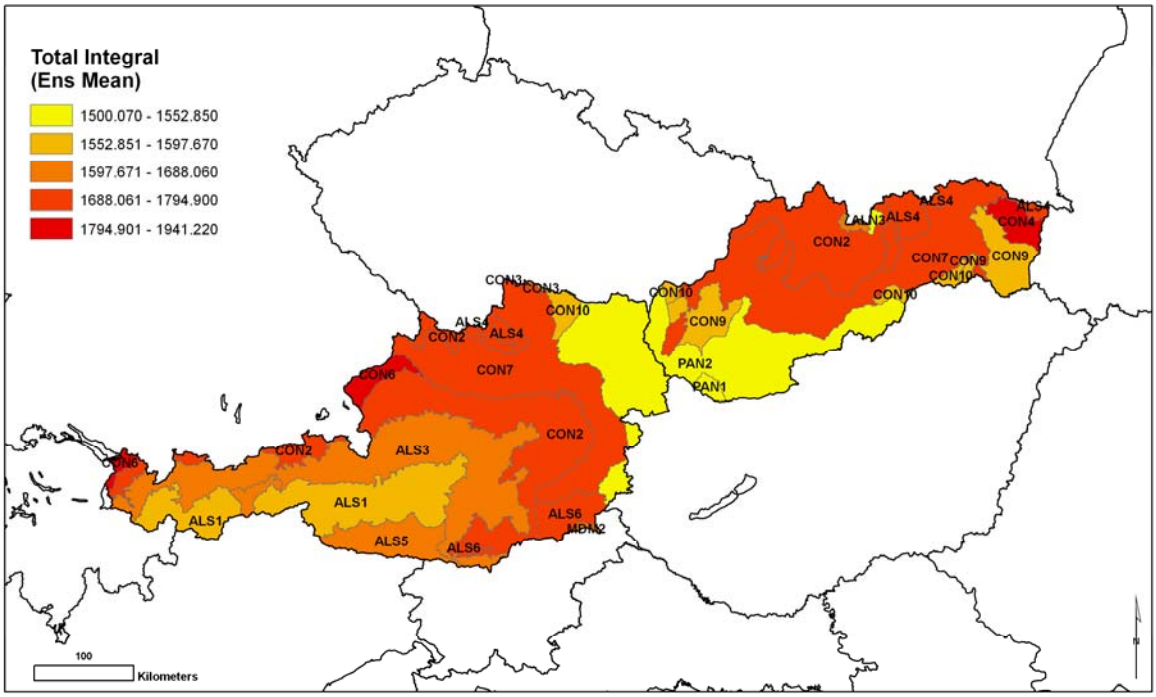

Figure 11. Distribution of Mean TI per Environmental Strata (SPOT NDVI data).

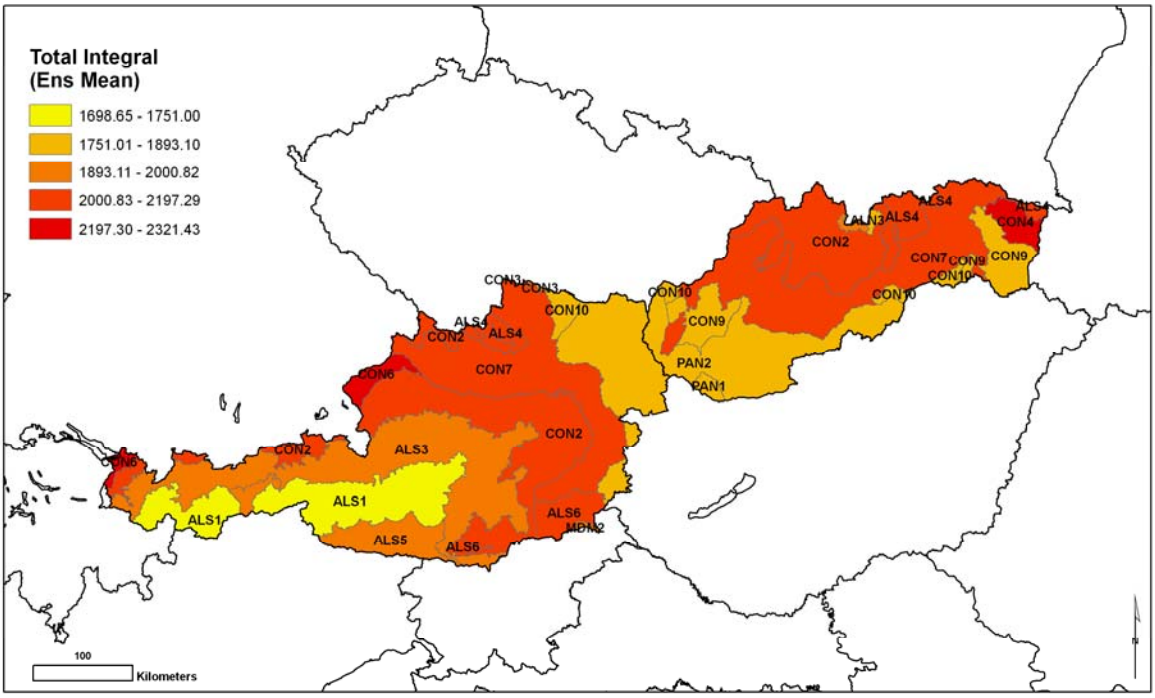

Figure 12. Distribution of Mean TI per Environmental Strata (MODIS NDVI data).

Table 5. Mean TI and standard deviation values per Environmental Strata (SPOT and MODIS NDVI data) and associated scatterplot (SPOT vs MODIS NDVI EnS average).

EnS	***SPOT***		***MODIS***	
	TI mean	*TI std*	*TI mean*	*TI std*
ALN3	1502.85	127.72	1790.38	325.77
ALS1	1576.64	158.39	1698.65	383.90
ALS3	1688.06	174.91	2000.82	352.39
ALS4	1751.05	121.98	2141.75	219.22
ALS5	1638.95	183.11	1947.87	349.48
ALS6	1783.27	113.31	2197.29	224.51
CON10	1567.54	142.39	1854.80	340.98
CON2	1785.30	145.01	2179.95	258.83
CON3	1597.67	84.57	1827.71	416.88
CON4	1886.28	91.26	2321.17	184.20
CON6	1941.22	146.94	2321.43	247.66
CON7	1794.90	136.49	2172.62	250.95
CON9	1564.38	152.33	1893.10	313.95
MDM2	1657.81	67.80	1981.04	246.08
PAN1	1500.07	87.02	1843.05	217.48
PAN2	1541.79	148.27	1815.30	330.15

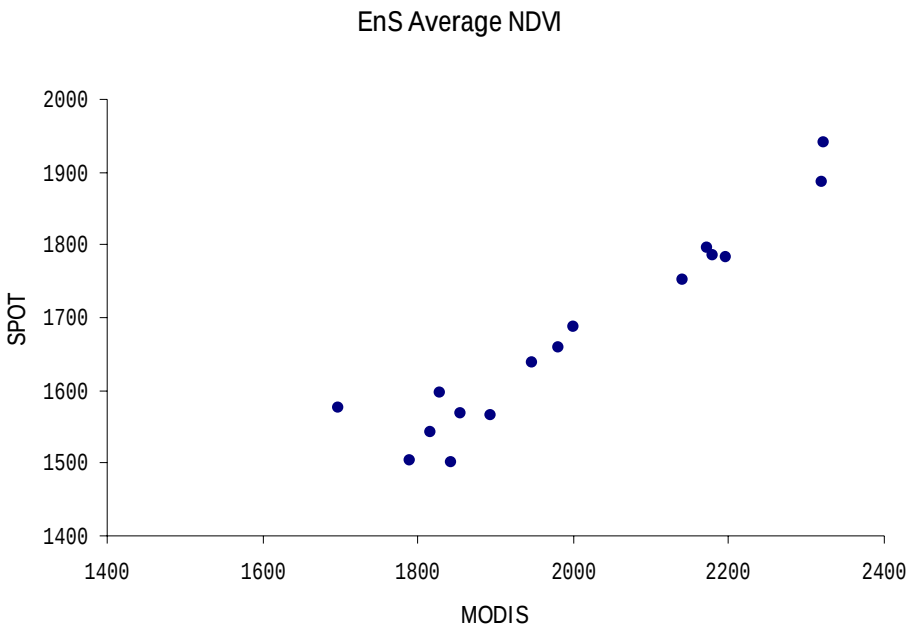

Peak of Season (NDVI Value)

The peak of season corresponds to the point of maximum NDVI along the growing season. We here show results for the MXV phenometric (NDVI value at peak of season). Although MXV mean values differ significantly between the two data series (see Table 6), they present similar spatial distribution (Figures below).

Low MXV values were detected for environmental strata ALN3 and ALS1 (Alpine areas), which are characterized by a higher proportion of bare soil/rocks, grass and sparse vegetation. These small values are possibly related to the amount and type of vegetation characterizing these strata (low density, higher proportion of herbaceous plants). Overall, higher MXV values belong to the Continental (CON) strata, dominated by broadleaf forests and on a second instance by agricultural areas. Data correlation between mean values of the MODIS and SPOT series is found to be high, with ρ = 0.94.

Table 6. Mean MXV and standard deviation values per Environmental Strata (SPOT and MODIS NDVI data) and associated scatterplot (SPOT vs MODIS NDVI EnS average).

EnS	*SPOT*		*MODIS*	
	MXV *mean*	MXV *std*	MXV *mean*	MXV *std*
ALN3	599.33	46.23	766.59	58.47
ALS1	625.12	52.33	752.79	69.09
ALS3	657.06	57.35	793.24	59.10
ALS4	723.75	48.12	841.97	39.55
ALS5	652.44	52.51	790.59	58.47
ALS6	730.33	21.20	848.39	22.68
CON10	701.48	47.15	808.07	55.74
CON2	700.68	43.79	832.26	37.24
CON3	686.39	30.03	783.56	27.35
CON4	798.10	37.15	889.98	35.07
CON6	706.46	27.68	822.67	33.70
CON7	731.50	50.94	843.08	48.16
CON9	700.93	45.77	819.85	48.01
MDM2	725.00	19.74	850.82	25.35
PAN1	683.17	28.24	819.53	42.38
PAN2	695.36	45.75	806.93	56.38

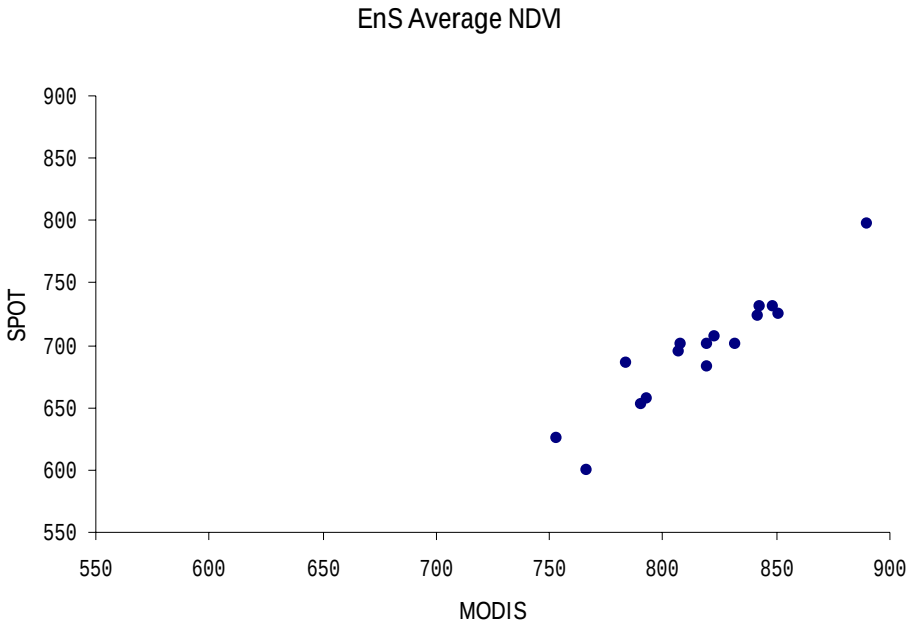

It should be noted that differences in wavelength centres and spectral windows of the bands relative to the SPOT HRV and MODIS sensors used in the calculation of NDVI values (VNIR and Red bands) produce differences in the raw NDVI values of the two sensors (NDVI MODIS always higher than SPOT). This means that an inter-comparison can be done, for example, relatively to the spatial patterns, but not on comparing single absolute values.

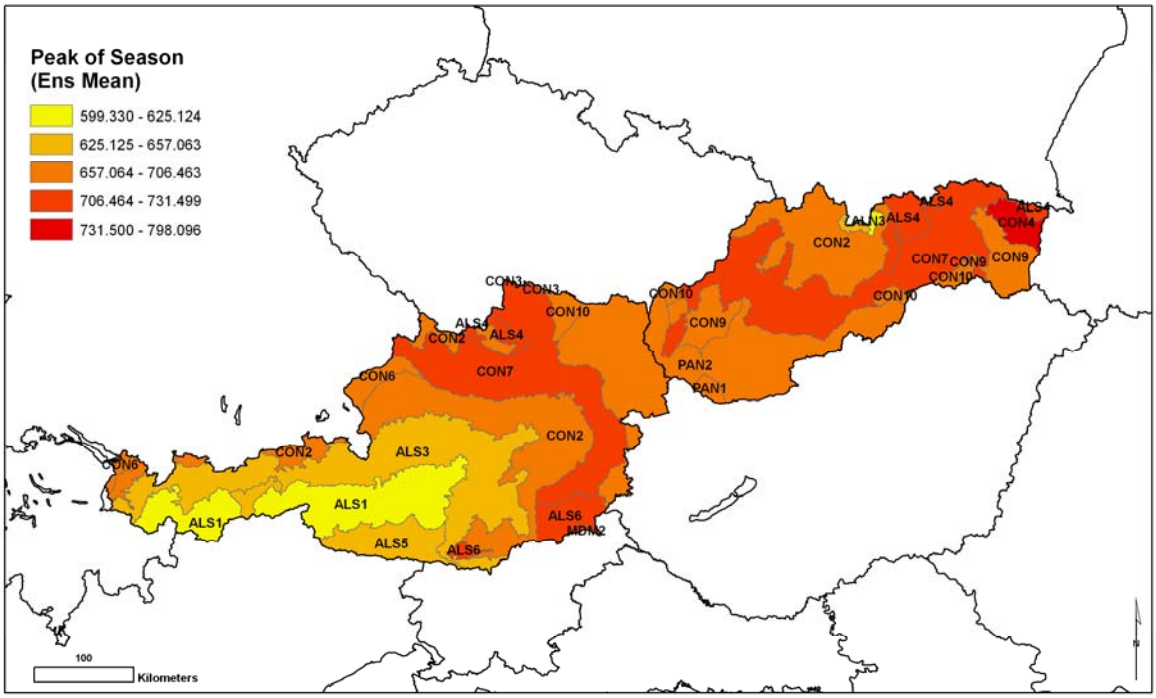

Figure 13. Distribution of mean MXV per Environmental Strata (SPOT NDVI data).

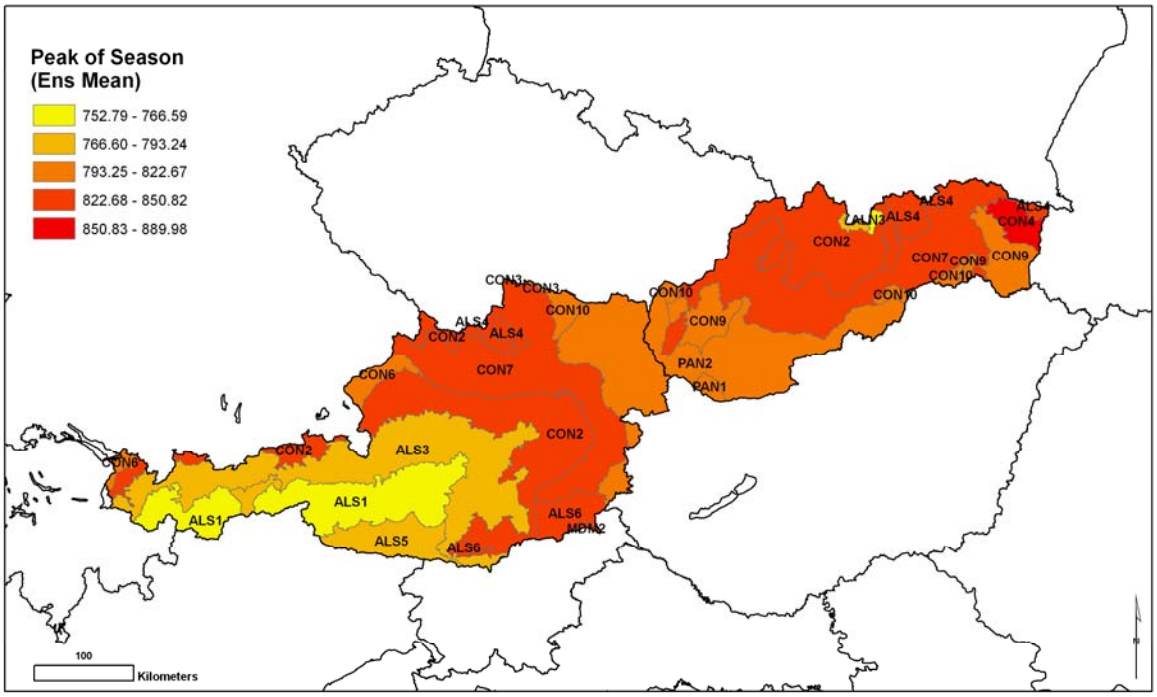

Figure 14. Distribution of mean MXV per Environmental Strata (MODIS NDVI data).

4.1.3 Forest Habitat classification using SPOT NDVI

Phenology information as extracted from remotely sensed VIs time series can provide valuable information to classify vegetation (see Steenkamp *et al.,* 2008; Geerken et al., 2005; Geerken, 2009). The following task was undertaken to investigate the use of Phenolo phenometrics to classify forest habitats. In this first section of the work pilot classification tests were performed based on time series of SPOT NDVI data at 1 km resolution. Random Forests (Breiman, 2001) is chosen as classification technique, having multiple advantages like being accurate, not sensitive to noise and computationally lighter than other classification methods. This approach has also produced promising results when applied to the classification of multisource remote sensing and geographical data (see Gislason et al., 2004).

The thematic level at which forest vegetation can be effectively mapped from medium-low resolution phenometrics is still an issue under investigation in the scientific community. Significant results were obtained mapping vegetation at the biome level using 1km AVHRR data (Wessels et al., 2011; Steenkamp et al., 2008). In the following methodology tests we focused on two lower ecological hierarchy levels for which data are available: *habitat* and *species*.

Mapping Natura2000 forest habitats

At the habitat level two Natura2000 habitat classes (see http://www.eea.europa.eu) were selected: the Medio-European limestone beech forests of the *Cephalanthero-Fagion* (Natura2000 code: 9150) and the Acidophilous Picea forests of the mountain to alpine levels (*Vaccinio-Piceetea*), code 9410 each of which represent respectively one of the most common broadleaved and needle leaved forest types in the area. This choice would enable us to establish whether the phenology of deciduous broadleaved and evergreen needleleaved forest is distinct enough to allow for a reliable classification based on phenometrics. No direct correspondence is present between Natura2000 and GHC habitat classification schemes; the focus of this section is a general testing of the methodology and processing chain.

Breiman (2001) defines the Random Forests as:
A classifier consisting of a collection of tree structured classifiers $\{h(\mathbf{x}, \Theta_k), k=1,... \}$ *where the* $\{\Theta_k)\}$ *are independent identically distributed random vectors, and each tree casts a unit vote for the most popular class at input* ***x****.* The collection of trees (‘forest‘) classifier finally

chooses the most popular class by combining all the 'votes' from the trees. Split within tree is based on a CART algorithm (Steinberg and Colla, 1995; Breiman et al., 1984).

Each tree is grown as follows:

- "If the number of cases in the training set is N, then sample N cases at random with replacement;
- If there are M input variables, then a number m<<M is specified such that, at each node, m variables are selected at random out of the M and the best split on these m is used to split the node (value of m kept constant during the forest growing).
- Each tree is grown to the largest extent possible. There is no pruning.

In our case, the M input variables were 31 phenometrics extracted for the study area. The Random Forests technique needs as input a number of reference samples, which are then internally split into a set of *training* samples and a set of *test* samples. The former provides the 'truth' information regarding the classes of selected habitats (2 in our case), while the latter is a set of points used to provide an estimate of error in the classification trees ('OOB Error'). In the Random Forests technique, there is no need for cross-validation or a separate test to get an unbiased estimate of the test set error, which is estimated internally during the run. For further details see Breiman (2001) and Gislason *et al.* (2004).

The Natura2000 GIS dataset is based on polygons with attributes related to shares (%) of priority habitats. First, it was tested if the share within delineated habitat site geometries (polygons) was sufficient to take the location into consideration for further classification and choice of training samples. Ideally, the polygon training samples had to be homogeneously covered with the one forest habitat class of interest. To achieve an adequate level of 'purity' in the reference polygon samples, three selection criteria were applied: 1) the habitat has an area share >60% within the polygon; or 2) the habitat has a percentage of <60% but >30% and it is the habitat with highest proportional share in the polygon. Finally, 3) all the extracted locations need to have a minimum share of 60% of CLC2000 (EEA, 2010) class Coniferous forest for Habitat 9410, and 60% class Deciduous Forest for habitat 9150.This latter criterion was added as the Natura2000 site geometry polygons share their percentage criteria attribute on large areas instead than on a pixel basis, data structure on which the classification and remote sensing data are based.
After selecting the initial reference samples, a Random Forests classification was performed using routines developed by Liaw and Wiener(2002) in R language.

Results and Discussion

The RF classifier was used to predict the distribution of the two selected priority habitat types in Slovakia (Austria was finally excluded due to scarcity of Natura2000 data). The parameters for RF were 31 variables (phenology indicators), number of trees = 500, m_{try} = 3 (initial number of randomly selected input variables, constant every node, determined using an in-built optimization step).

The extraction of training pixels led to an equally distributed population between Habitat 9150 (n=214) and Habitat 9410 (n=256). The inbuilt accuracy assessment, which is calculated on approximately ⅓ of independent data (test samples), resulted in an error estimate of 0.65 % in the choice of the two habitat classes (9410 and 9150); in other words, pure pixels were classified correctly in 99.35% of the cases. A Confusion Matrix is presented in *Table 7.* It should be noted that that the training and test samples (1km pixels) are located within the Natura2000 polygons, which covers a small percentage of the study area. This could influence the accuracy results.

A significant feature of the RF technique is to provide an estimate of the importance of the phenology variables used in the classification, in other words RF calculates which phenometrics contributed more to the classification result and which one were less influent. This is estimated by looking at how much the prediction error increases (OOB) when data for that variable is permuted while all others are left unchanged. *Figure 15* below shows the phenometrics used in the classification sorted for importance –Mean Decrease Accuracy- (see *Table 1* for variable ID and meaning). In this test the more influent phenometrics in the classification accuracy resulted: Peak of Season-value (MXV), Normalized Season and Growing Integral (SNI, GNI) and value of Growing Season End (GEV).

The RF classification results showing the predicted probability of a pixel being classified as habitat 9150 (Acidophilous Picea forest) or habitat 9410 (Limestone beech forest) was mapped in a GIS environment (*Figure 16*). The spatial distribution of the inferred habitats was compared qualitatively with the results obtained from the Habitat maps produced by Mucher *et al*. (2009). *Mucher et al.*(2009) created a series of predicted habitats maps based on the integration of ecological knowledge with available European datasets of land cover and site conditions.

Table 7. Confusion matrix of Natura 2000 Beech and Picea pure pixels classification.

	Beech	Picea	*OOB Error*
Beech	213	1	0.0046
Picea	2	248	0.0080
OOB estimate of error rate: 0.65%			

The maps shown in *Figure 16* indicate generally a good agreement between the Random Forest classification and the Mucher *et al.* (2009) predicted distributions, showing similar general patterns for both maps at regional scale. However, Habitat 9150 is slightly underestimated in the RF classification with respect to the results of Mucher *et al* (2009), and a South western patch of *Pinus silvetris* was misclassified as *Picea* forest A more rigorous comparison between the two maps would need a better harmonization between compared data (e.g. regarding threshold probabilities, see Legend in *Figure 16*). The map generated using the RF classification uses only remote sensing time series and no ancillary data such as climatic, geological/soil data or topographic information as in Mucher et al. (2009) model.

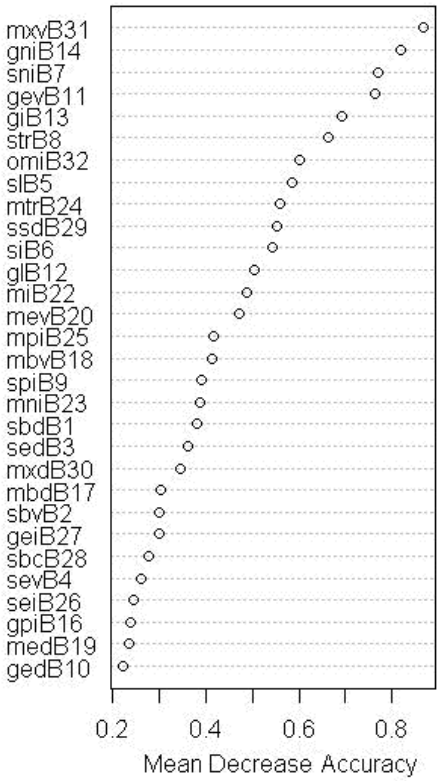

Figure 15. Phenometrics sorted by the importance in contributing to the classification accuracy (Acronyms in *Table 1*).

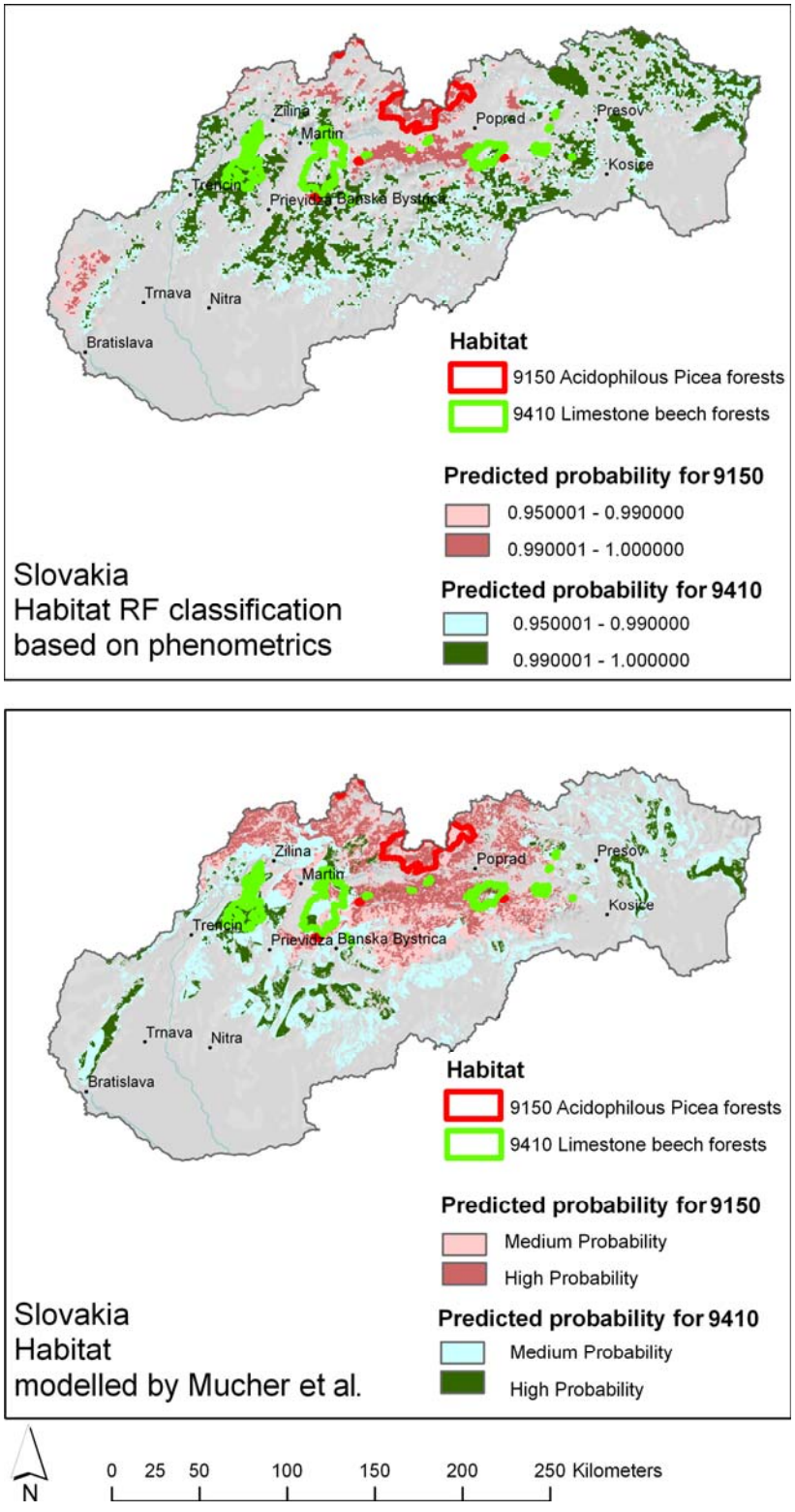

Figure 16. RandomForests habitat classification based on phenometrics (upper figure) and the habitat prediction model by Mucher *et al*. (2009), lower figure. Habitat polygons source for training: Natura2000.

Tree species classification

A Random Forests classification based on SPOT NDVI phenometrics was carried out using forest tree species distribution data. The exercise was performed to test the performance of the classification technique using phenology information to deliver a thematic classification level which is more detailed than the habitat level, i.e. species. The data used belongs to the AFOLU Tree Species distribution maps, developed by EC JRC (Koeble and Seufert, 2001). The Dataset is composed by 137 tree species distribution maps at a 1km resolution. The data was derived by modelling information from four Pan-European datasets: 1) Land cover from CORINE; 2) Land cover from PELCOM (Pan European Land Cover Mapping) for areas where no CORINE data was available; 3) Species information from ICP Forest Level I; and 4) statistical data from the FAO-TBFRA2000 (Temperate and Boreal Forest Resources Assessment 2000). For this analysis, the study area included both Slovakia and Austria.

The assessment focused on three common species in the study area: *Fagus sylvatica, Picea abies*, and *Pinus sylvestris.* The tree species reference data were derived from the AFOLU database by applying the following criteria for the extraction of 'pure' pixels:

- pixel is classified as one of the selected tree species;
- one of the three species is present in more than 60 % of the pixel area (attribute in the AFOLU database).

A subset of pixels was then randomly chosen to be used as classifiers. Their number varies depending on the abundance of the tree species in the study area (*Table 8*). For this classification the number of phenology indicators used in the RF was reduced to 24. This number was chosen after performing a first run of the classification with 31 phenometrics and eliminating from the second run the 8 phenometrics with the least impact on the classification accuracy results. Doing this led to a lower OOB error. The number of trees was set equal to 500 and m_{try}= 4 (initial number of randomly selected input variables at each node).

Results

The accuracy assessment of the classification resulted in an overall OOB error of 17.6 % on the determination of the three tree species. A confusion matrix is produced and reported below (*Table 8*).The higher classification error for *Pinus sylvestris* is due to a high occurrence of 'low purity' pixels, as observed in *Figure 18*, left. The RF predicted probability of tree species presence was mapped in a GIS environment, and the spatial distribution compared qualitatively with the AFOLU data (*Figure 19*).

Table 8. Confusion matrix of the tree species RF classification, and number of training points used (n).

	Pinus sylvestris	*Picea abies*	*Fagus sylvatica*	*OOB Error*	*n (training points)*
Pinus sylvestris	233	174	93	**0.534**	500
Picea abies	56	1860	84	**0.070**	2000
Fagus sylvatica	27	182	791	**0.209**	1000

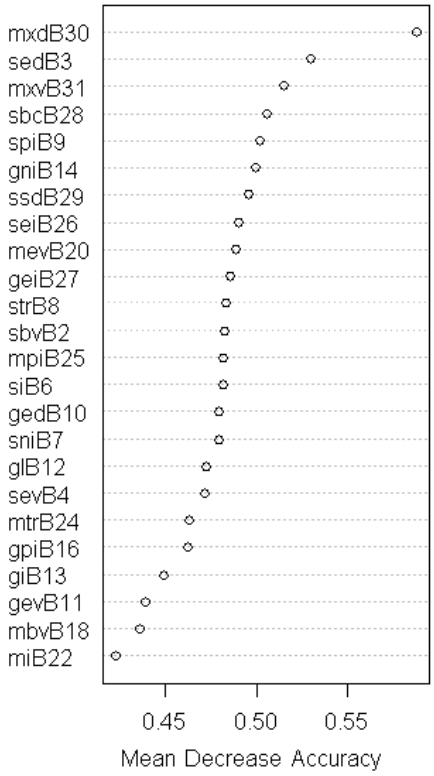

Figure 17. Phenometrics sorted by the importance in contributing to the RF classification (Acronyms in *Table 1*).

A comparison between the two classification data was produced using scatter plots (*Figure 18*). In order to reduce noise, the original maps of 1 km grid size have been aggregated to 3 x 3 km grids and linear correlation coefficients calculated. Pearson's correlation coefficient (R) is calculated between the predicted probabilities of belonging to a class versus the observed area share of the pixel (AFOLU) for that class. Provided this assumption is a simplification (assuming the area share is equivalent to a presence probability in the pixel, see Hill et al., 2007), the coefficient reveals some accordance between the datasets, especially for *Pinus* and *Fagus.* A good spatial agreement is also qualitatively observed, especially for the Alpine strata -AL- and the CON2 stratum (Continental 2).

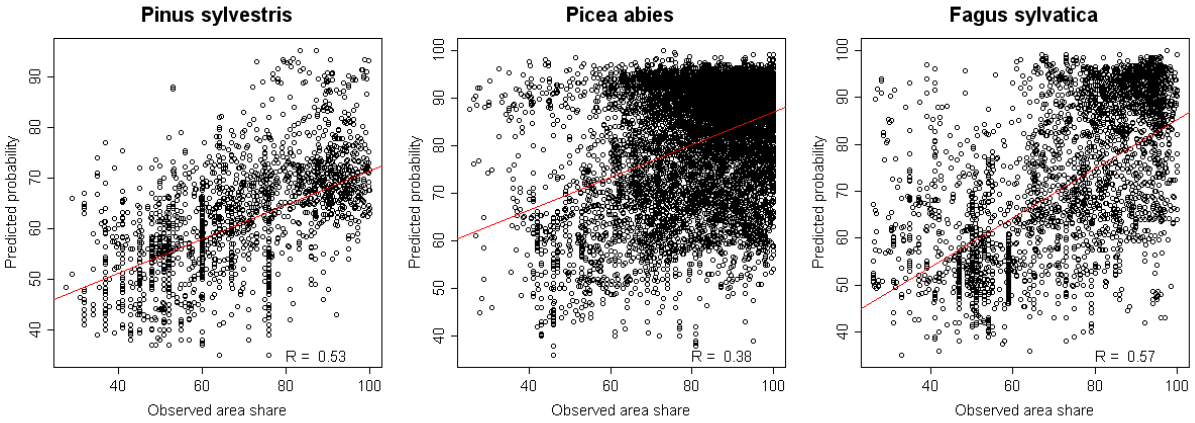

Figure 18. Scatter-plots and R coefficients for mean aggregated (3 by 3 km) values of AFOLU data (area share) and predicted tree species probability of RF classification. Only pixels of dominant species probabilities and those greater than 25 % of area share are shown.

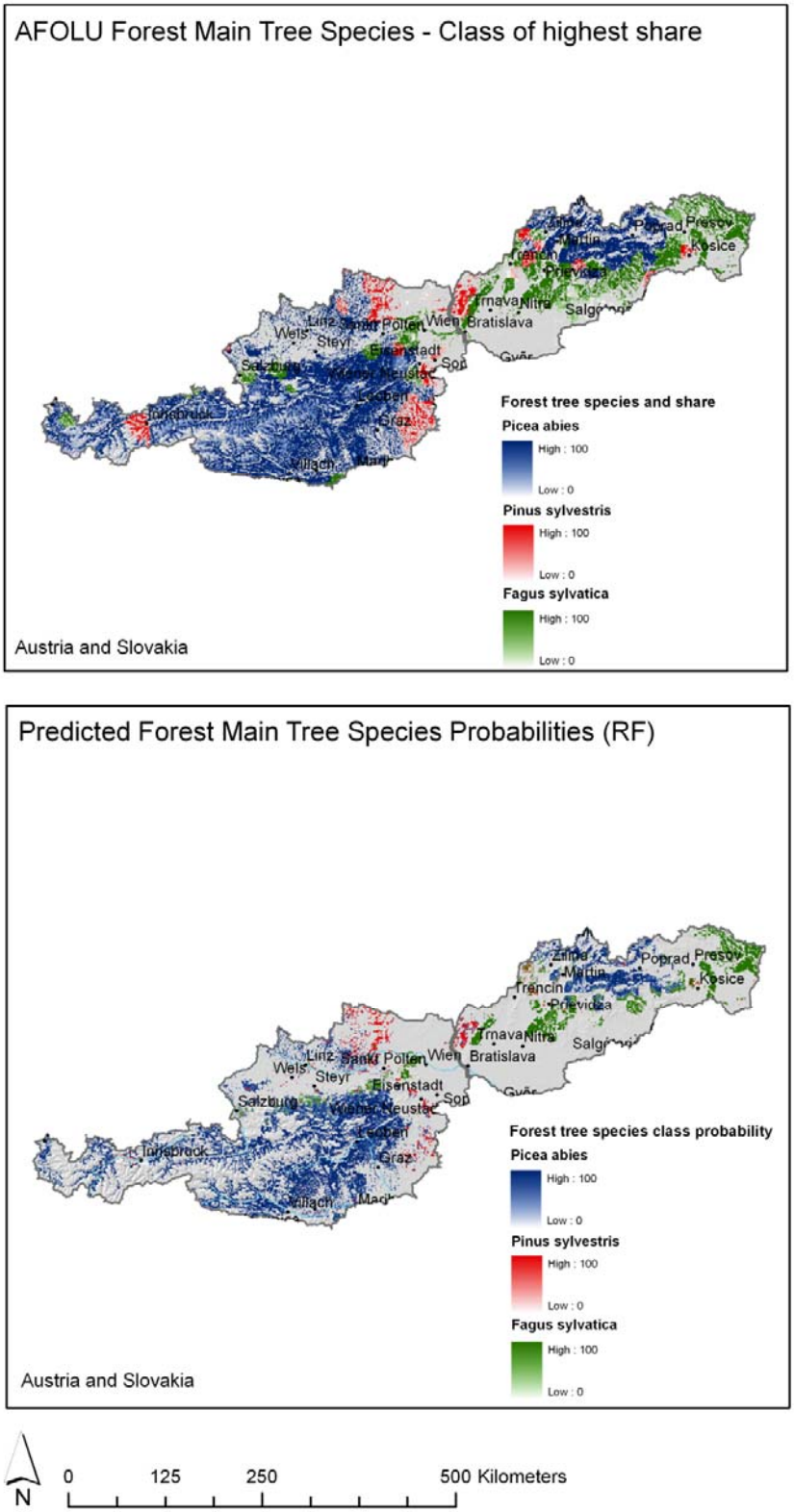

Figure 19. AFOLU map of the selected tree species -highest share class- (Koeble and Seufert, 2001) and RF tree species classification based on phenometrics (lower figure).

4.2. Classification using MODIS NDVI Data

4.2.1 Introduction

After pilot testing the general methodology, the analysis focused on MODIS NDVI data as this data set was deemed more adequate because of its spatial resolution (250 m): the higher spatial resolution was expected to reduce the number of mixed ('unpure') pixels and thus lead to better classification results. This time Austria was selected as the initial study area, which in a second step was extended to a selected Environmental Zone (Metzger et al., 2005).This time the thematic level tested was the habitat level and the adopted classification system determining the EO derived forest habitat classes was the *General Habitat Category classification system* (Bunce et al., 1998; 1996), which is the classification scheme adopted by EBONE.

Forests in the GHC system are categorised as the Forest Phanerophytes (FPH) class, which is defined as woody vegetation with a minimum height of 5 m. The following (leaf) forms allow for a further subdivision: Forest coniferous (FPH/CON), Forest deciduous (FPH/DEC) and Forest evergreen (FPH/EVR) classes. Detailed information on the rule based system adopted to establish which habitat and phyto-sociological vegetation association is grouped in FPH is found in Bunce et al. (2010).

4.2.2 Field data

As discussed, the Random Forests technique needs as input a set of training pixels to run the classifier ('pure pixels'). This information is extracted from 1 km x 1 km plots sampled and classified in the field by EBONE partners, or from existing field samples, translated into the GHC scheme (see *Table 9*). Available field plot data are located in Austria, Italy, Southeast France and Sweden. Field data from Sweden were in some cases discarded from the analysis as the NDVI time series in this regions affected by large periods of missing data (prolonged cloud coverage, snow, etc).

The plot data were provided as ESRI shapefiles, classified under the GHC scheme. Polygons with FPH/CON,FPH/DEC and FPH/EVR attributes were selected and overlapped with the 250 m raster grid structure of MODIS NDVI data. A pixel was considered as 'pure' if the proportion of CON, DEC or EVR was greater than or equal to 70% within the MODIS pixel (see *Figure 20*).A very limited total of 81 pure pixels were identified (51 CON and 29 DEC).No pure pixels for the GHC EVR were found.

Table 9. GHC field plots description.

Country	*#Plots*	*Organization/Project*
Austria	48	University of Wien/SINUS
France	11	EBONE/PYRODIV
Sweden	25	NILS
Italy	15	BioHab
Sum	99	

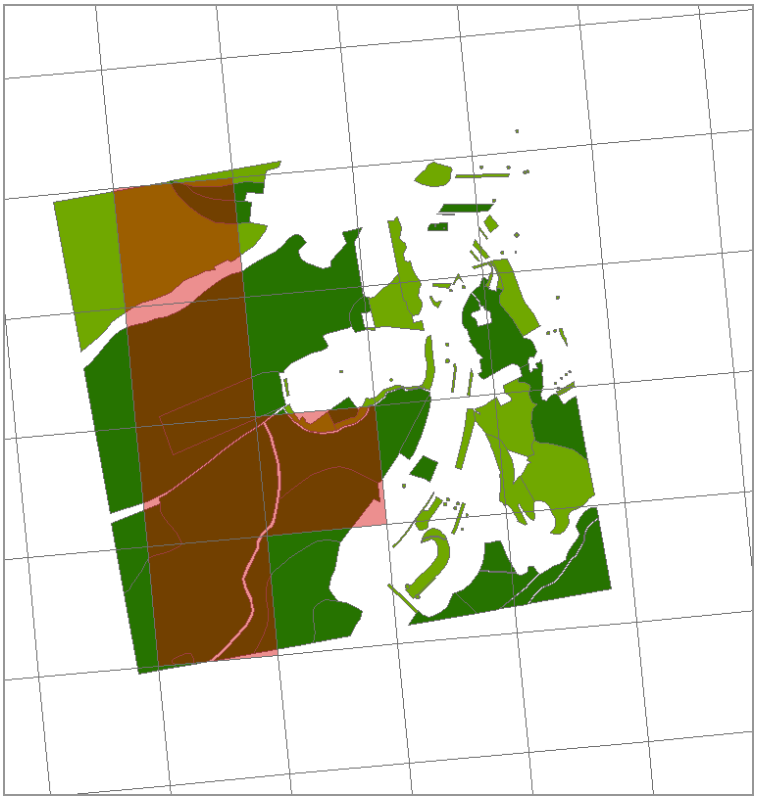

Figure 20. FPH polygons (dark and light green) were overlapped with the MODIS NDVI grid to extract 'pure' MODIS pixels (in red).

4.2.3 Classification of coniferous and deciduous forests (GHC)

Austria

The first part of the MODIS data analysis was to investigate the performance of the RF classification using NDVI phenometrics to detect forests under the GHC scheme. Two forest types were considered: coniferous (CON) and deciduous (DEC).The test area was initially limited to Austria. To understand the relationships between the number of phenometrics and the ability of the RF classifier to discriminate Coniferous and Deciduous forest, 29 recursive

classification tests were launched using the 48 'pure pixels' reference plots. At every cycle *(1+n)* phenometrics were excluded, where *n* varies from 0 to 28 and the Mean Decrease Accuracy (MDA) calculated. MDA is a measure provided by the RF algorithm that quantifies the decrease in classification accuracy when eliminating one of the phenometrics from use in the classification.The MDA is used to determine the relative contribution of each phenometric to the classification. The type and number of phenometrics were selected by ranking the phenometrics according to MDA (*Figure 21*). For each of these classification tests *100* runs were performed.

In this test the OOB error decreases by performing classifications with the phenometrics listed at the top of the MDA graph (*Figure 21)*, while adding phenometrics listed at the bottom of the MDA graph led to decreased ability of the classifier to discriminate CON and DEC pixels in the training set (monotonic relationship statistically significant based on Spearman's rank correlation coefficient: Figure 22). The four most relevant phenometrics in this classification test are all *date* phenometrics (MXD, MEV, MBV, SBV).

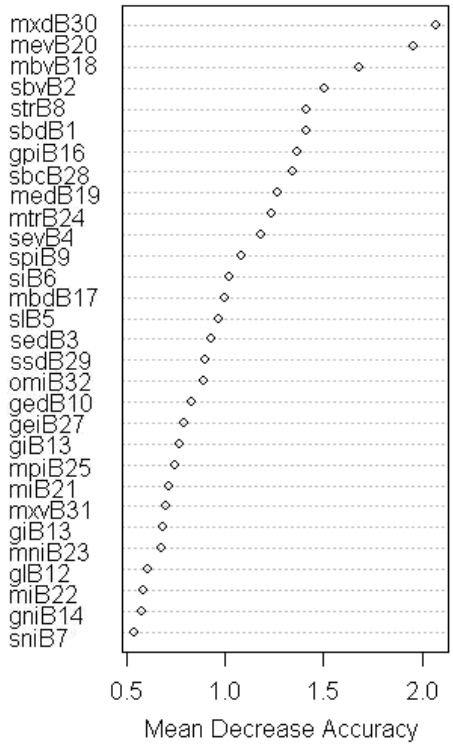

Figure 21. Mean Decrease Accuracy using all phenometrics for CON and DEC classification (Austria).

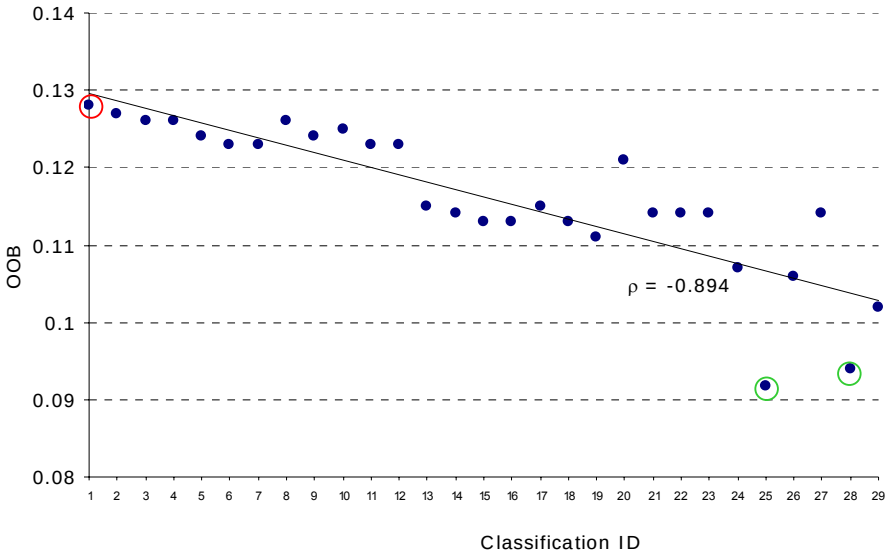

Figure 22. Ability of the RF in discriminating pure CON and DEC pixels among MDA-ordered phenometrics configurations (red circle: higher OOB; green, lower).

The lowest OOB errors were obtained using the phenometrics configuration in Ph28 (OOB=0.094) and Ph25 (OOB=0.092), while the highest error was obtained using all phenometrics except one: Ph1 (OOB=0.128).These three phenometrics configurations (Ph1, Ph25, Ph28) were used to run RF classifications in Austria to compare the classification performance for GHC Coniferous and Deciduous forests. The classifications were carried out on a subpopulation of the 250m MODIS NDVI pixels defined by extracting within the 25 m JRC Forest Mask 2006 (Kempeneers et al., 2010) those pixels that have at least a 70% share of CON or DEC (the latter correspondent to 'broadleaf' in the Forest Mask 2006 dataset). This operation (i.e. removing pixels not classified as forest in any of the two datasets) was performed to get a fully comparable dataset when evaluating classification accuracy. *Figure 23* shows a map of the RF classification using the Ph28 configuration and the JRC Forest mask 2006data upscaled at 250 m. The outcome of the RF classifications is pixel base maps containing for each forest pixel the probability of it being CON or DEC.

A) Forest Classification using the Ph28 configuration

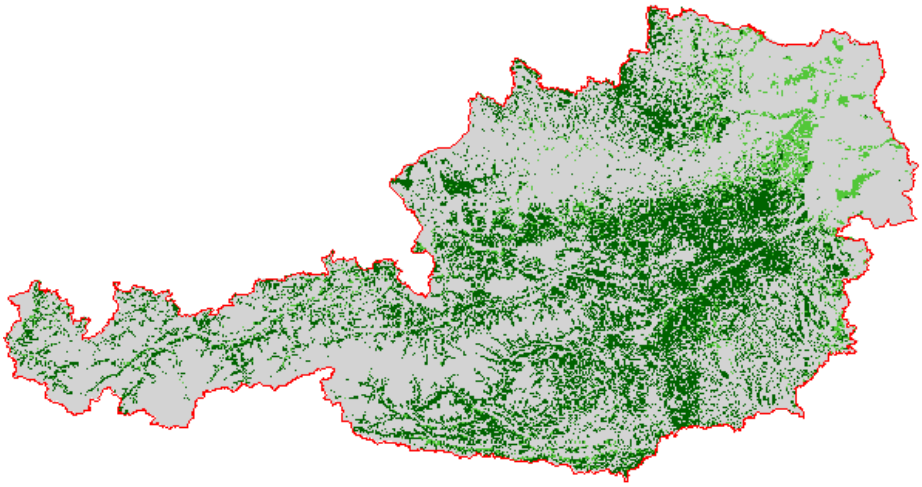

B) Forest layer from the JRCForest Mask 2006 at 250 m

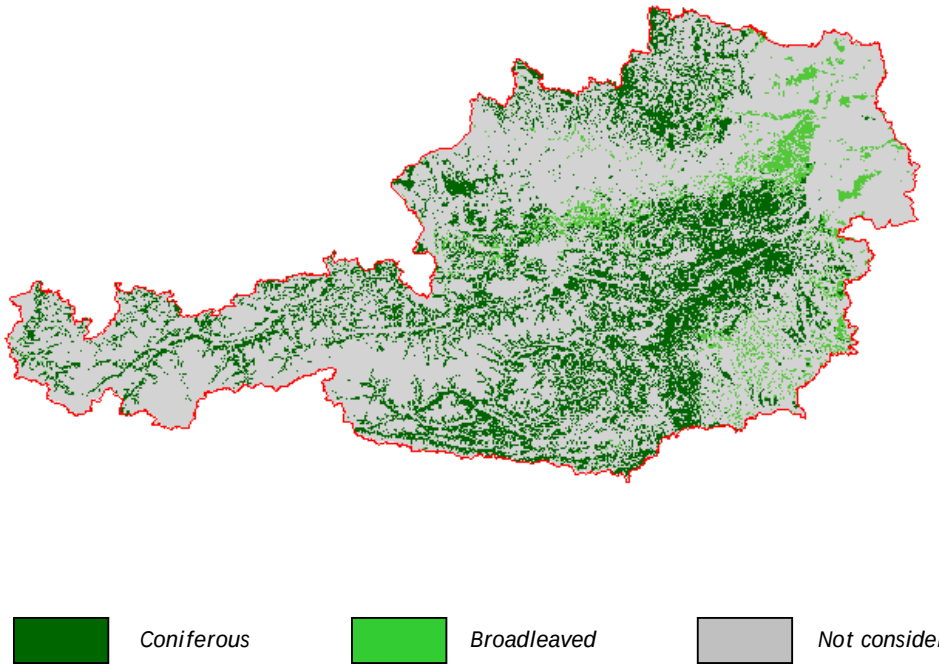

Figure 23. Forest Classification based on Random Forests using the Ph28 configuration (upper image), and the Forest layer derived from the JRC Forest Mask 2006 (lower image). Both images are at 250 m.

Accuracy Assessment

An assessment of the overall accuracy of the three RF classifications (Ph1, Ph25, Ph28) was performed using the JRC Forest Cover Map 2006 (Kempeneers et al., 2010) upscaled at 250 m. The JRC Forest Cover Map 2006 provides coverage for Europe at a 25 m resolution. It was derived using IRS-P6 LISS-III, SPOT4 (HRVIR) and SPOT5 HRG imagery for the years 2005-2007.The overall accuracy of the JRC Forest Cover Map 2006 was reported to be higher than 85% (Kempeneers et al. 2010). For more detail on the used classification algorithms and processing chain see Kempeneers et al. (2010). The GHC categories considered by the RF classifications are comparable with the ones defined by the JRC Forest Cover Map 2000 (see *Table 10*; Pekkarinen et al., 2009).Two forest classes are present in the JRC Forest Cover dataset: *broad-leaved* and *coniferous*. The broad-leaved class contains Deciduous and Evergreen types, the latter being negligible in Austria thus allowing a direct comparison with the broad-leaved forest class of the RF classifications. .

The JRC Forest Cover Map 2006 dataset was adopted for multiple reasons: 1) it has a pan European coverage, thus allowing inter-comparisons across a wide range of study areas in Europe, 2) it covers a period included in the MODIS NDVI time series, and 3) it is the only recent European dataset holding Broadleaved/Coniferous forest type information.

The validation dataset was derived from the JRC Forest Map 2006 as follows:

- The JRC Forest data was summarized to match the spatial resolution of the MODIS NDVI raster grid (250 m) by calculating the proportion of 25 m forest class pixels present within each 250 m pixel;
- The validation set was created by selecting the 250 m pixels with a proportion of either Coniferous or Broadleaved forest ≥ 70% and classing those as CON and DEC respectively.

The accuracy assessment was performed by carrying out a pixel based comparison between the validation data set and the Random Forests CON and DEC class assignments of Ph28, Ph25, Ph1which were determined by assigning to the pixels the class with the highest *p* value (e.g. if p_{CON} = 0.51 the pixel is classed as CON). *Figure 24* summarizes the accuracy assessment scheme.

Vegetation types
Broad-leaved - broad-leaved forest with more than 30% crown cover - plantations of e.g. eucalyptus, poplars - evergreen broad-leaved woodlands composed of sclerophyllous trees (mainly *Quercus ilex, Quercus Suber, Quercus Rotondifolia*) - arborescent mattoral with sclerophyllous species -olive-carob forests dominated by *Oleaeuropaea sylvestris, Ceratonia siliqua* - palm groves woodlands, tamarix woodlands, holly woodlands - broad-leaved wooded dunes - sub-arctic broad-leaved forests not reaching the 5 m height - transitional woodland areas when the canopy closure of trees cover more than 50% of the area and if their average breast height diameter is at least 10 cm. Coniferous: - coniferous forest with more than 30% crown cover - non-evergreen coniferous trees woodland composed of *Larix* species - arborescent mattoral with dominating *Juniperus oxycedrus/phoenica* - Christmas trees plantations - coniferous wooded dunes - sub-arctic coniferous forest, not reaching the 5 m height. Mixed: - mixed forest, the share of coniferous or broad-leaved does not exceed 25% in the canopy closure - mixed wooded dunes.

Table 10. Categories included in the forest class of the Forest Cover Map 2000 (from the Forest Action Website, 2010).

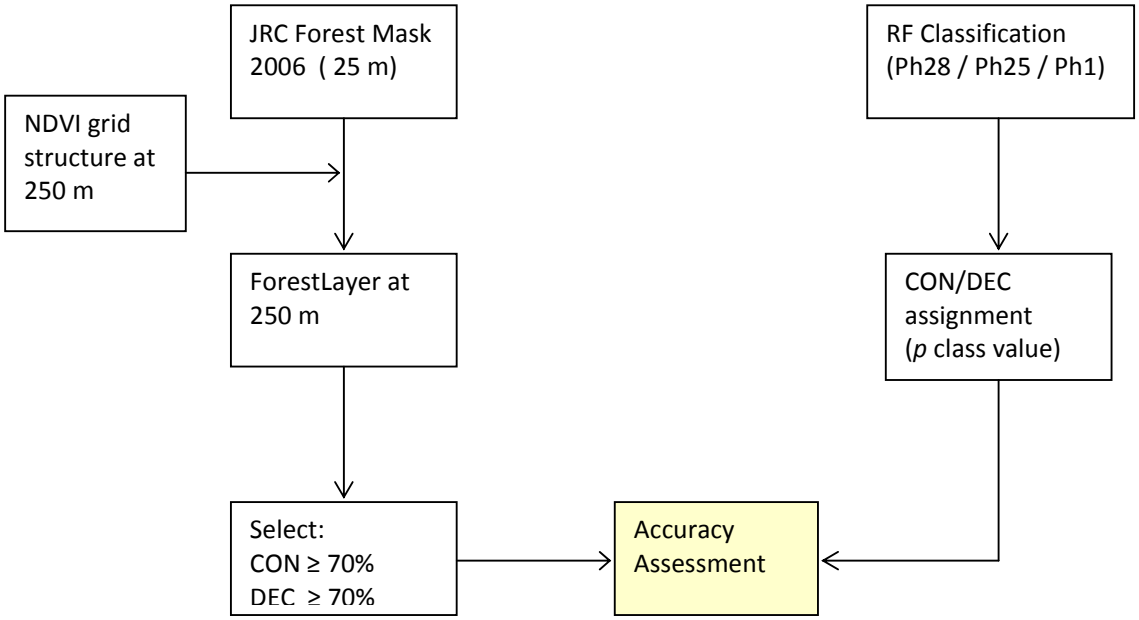

Figure 24. Flow chart of the Accuracy Assessment scheme used.

Class and overall mapping accuracy for the three RF classification configurations are reported in Table 11.

Table 11. Class and overall classification accuracy for Ph28/ Ph25 / Ph1 configurations.

Class Accuracy (%)	***Ph28***	***Ph25***	***Ph1***
Coniferous – CON	82.18	82.39	76.70
Deciduous – DEC	37.31	36.55	29.65
Overall Accuracy (%)	83.89	84.01	78.78

Low accuracy values in the deciduous class can be due to a series of reasons, among them the vegetation type heterogeneity of the class which will cause the phenometrics values of the class to vary substantially.

The area with the highest discordance between the RF classifications and the reference dataset is located in Southeast Austria (Graz region). Here forest types are characterized by *mixed* formations, as observed using CLC2000 data and regional maps (vegetation map from Austrian *Institut für Waldinventur, http://bfw.ac.at/rz/bfwcms.web?dok=4636*). To investigate if the GHCs forest classification accuracy can be improved we introduced the presence of a mixed class in the RF scheme. The mixed class is defined with the following rule: a pixel should have a proportion of FPH/CON < 70% or FPH/DEC <70% but their sum is greater or equal to 70% of forest–FPH- (the adopted definition of forest pixel is when it is included at least 70% share of forest type). This defines a new population of 'pure pixels' for the mixed forest class. The Ph25 phenometrics configuration was selected for comparison, having achieved the best overall accuracy in the previous assessment.

A Random Forests classification with the three forest classes was run for Austria. The accuracy assessment is performed using CLC2006 data (from EEA, www.eea.europa.eu) at 250 m as the reference data set, including the land cover classes broad-leaved forest (class 311), coniferous forest (class 312) and mixed forest (class 313). Accuracy results are shown in the following table.

Table 12. Class and overall accuracy for Ph25 configuration after introduction of the mixed class.

Class Accuracy (%)	***Ph25***
Coniferous – CON	79.03
Deciduous – DEC	44.54
Mixed – MIX	21.31
Overall Accuracy (%)	75.77

Discussion

The RF classification using pure forest classes in Austria revealed satisfactory results for the classification of coniferous vegetation (FPH/CON), while low performance is found in classifying deciduous forest (FPH/DEC). Low accuracy values of the latter are likely to be caused by a higher variability in the time series characteristics of this class, which is reflected in the phenology indicators variance. *Figure 25A* shows for example, the presence of higher fluctuations of NDVI signal in winter decades for the pure deciduous points. In the contrary, coniferous forests show generally more homogeneous inter-annual runs. The satisfactory value of the overall mapping accuracy is due to the unbalanced proportions of coniferous and deciduous pixels, the former being much more abundant in Austria, and increasing the overall accuracy.

The introduction of a mixed class decreased the overall classification accuracy and the accuracy of the FPH/CON class. The FPH/DEC showed a slight increase in accuracy. The construction of this class based on theoretical assumptions of CON-DEC mixtures could have introduced a form of class 'noise' negatively affecting the classification accuracy. Also, unexpected trends in the time series of the pure training pixels for the MIX forest class are present: NDVI values in the summer decades are occasionally higher than the CON and DEC classes (*Figure 25A*). This may suggest that the training data set may not be fully suitable. A control profile using a random set of points in Austria from CLC2000 forest classes (Coniferous, broad-leaved and mixed) showed a different and more reasonable trend (*Figure 25*B*).*

Two remarks can be drawn:

- RF classification accuracies showed inverse proportionality with OOB errors, calculated on training (pure) pixels. The Out Of Bag error is an indication which helps to discriminate worst and best phenometric configurations. In the presence of correlated variables and well distinguished pure pixels, the OOB error can help to address a more efficient classification. This is not to be taken as a general rule, but should be checked on:1) site specific basis and 2) it can vary depending on phenometrics correlations.

- Mean Decrease Accuracy (MDA) can help understand which phenology indicator would better contribute to discriminate the two forest classes. On the other hand, MDA is calculated with respect to the training pixel group. The variance present in non pure data can potentially provide different MDA behaviour. Inference of these conclusions to the general case needs further investigation at pan-European level.

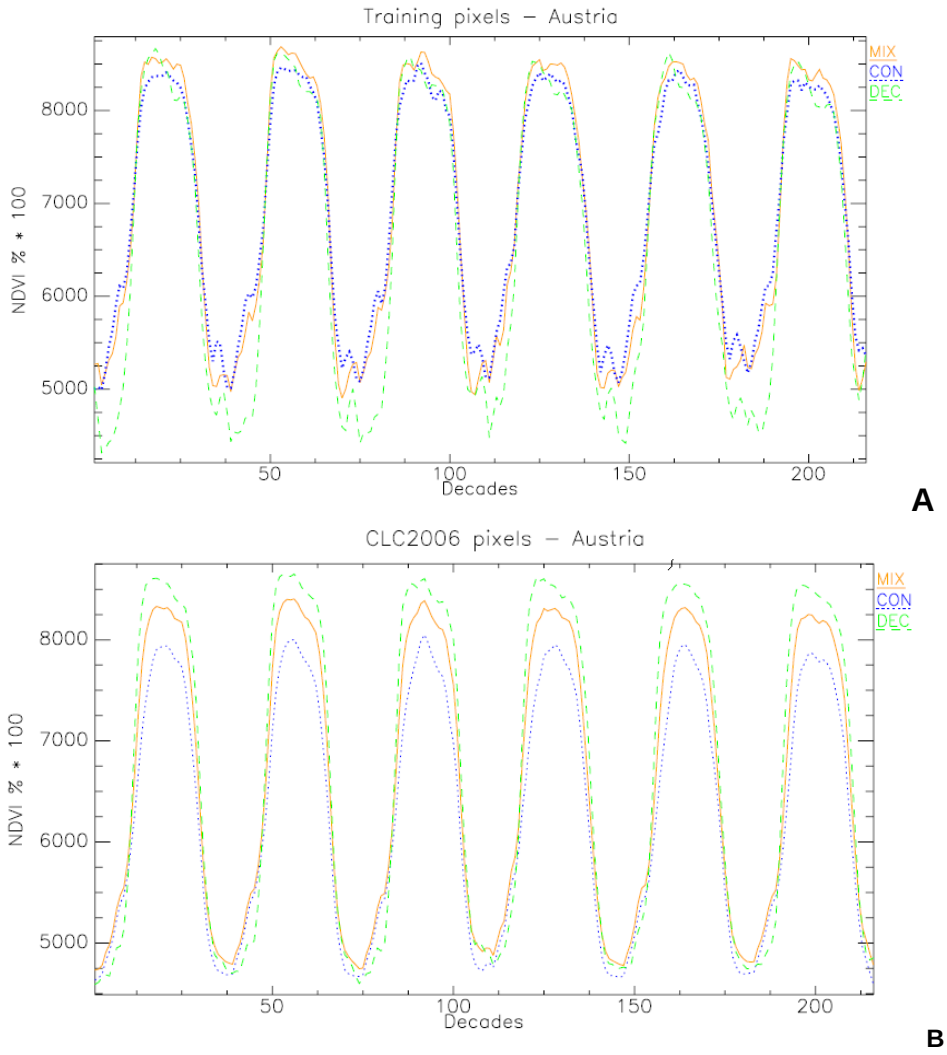

Figure 25. NDVI interannual run for pure pixels of CON, DEC and MIX classes (A: GHC training pixels. B: pure pixels from CLC2000).

Mediterranean Environmental Zone

The same classification steps described in the previous section where performed for a region dominated in this case by broadleaf forest (Mediterranean Zone, MDN in *Metzger* classification). The three phenometrics configurations chosen are Ph28 (excluding 28 indicators), Ph14 and Ph0. These were selected to represent 'extreme' situations in terms of phenometrics number, plus a middle configuration. In this way we wanted to test a configuration criterion independent to the analysis of OOB errors. A total of 30 training pixels were selected within the MDN zone. Only FPH/CON and FPH/DEC pure pixels were available, while no pure FPH/EVR were found in the available data (DEC and EVR were considered as a single class). Three RF classifications of FPH Coniferous and Deciduous

forests were performed (no mixed classes), with trees number=500 and m_{try}=4. Also in this case, the subpopulation of pixels on which the classification was applied was defined by selecting those 250m pixels that have at least a 70% share of coniferous or 70% of broadleaved forest (the within pixel proportion of coniferous and broadleaved forest was calculated using the 25 m JRC Forest Mask 2006, as described in *Section 4.2.2*). As discussed, this operation is added to eliminate mixed pixels from the validation dataset, focusing on 250 m pixels representing a dominant vegetation type. *Figure 26* shows the classified image using all phenometrics (Ph0).

An accuracy assessment following the same processing chain described in *Figure 24* was performed. Class and overall mapping accuracy for the three classification configurations are reported in Table 13.

Table 13. Class and overall classification accuracy for three phenometrics configurations in the MDN Environmental Zone.

Class Accuracy (%)	***Ph28***	***Ph14***	***Ph0***
Coniferous – CON	34.84	38.65	47.65
Deciduous – DEC	52.96	54.30	58.01
Overall Accuracy (%)	**62.41**	**64.52**	**69.62**

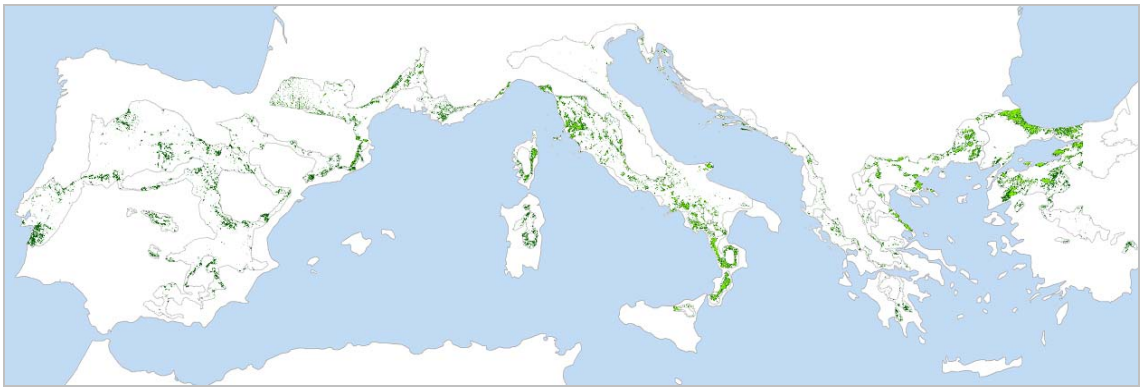

Figure 26. RF classification map of forest types using the Ph0 configuration (MDN Environmental Zone). Dark green Coniferous (FPH/CON) and light green Deciduous (FPH/DEC).

Discussion

All RF classifications performed in the MDN Environmental Zone showed low classification accuracy, which are much inferior to the levels achieved for Austria (Table 11). These results are potentially produced by a series of factors, among them the pixels employed to train the

RF classifier, and the validation dataset used. In the classification accuracy assessment we used as reference the JRC Forest map 2006 (Kempeneers et al, 2010). This dataset is derived using a spectral classification approach, while the classes identified in the GHC field plots are built based on field observation. The former made use of medium resolution (30/250 m) imagery information, classified using training pixels extracted from the CLC2000 map; the latter is based on *in situ* assessment of forest type, their density and life forms.

Two important considerations should be made about the two different approaches:
1) 'Pure pixels' from GHCs field plots were defined based on thresholds of class share within the MODIS pixel (see *Figure 20*).Visual observation of the FPH/CON and FPH/DEC training pixels using the *GoogleEarth*® interface showed that a GHC forest class often shows differences in spatial characteristics of the vegetation cover. This is due to local vegetation characteristics (e.g. forest density, species), together with the influence of the non-tree background. Such differences are likely to have an impact in the spectral signature of the training pixels. As illustrated in
Figure 28*A*, GHC FPH/DEC polygons overlapped on high resolution images show heterogeneity in terms of tree density and background extension (see for example the zoomed inset). Figure 27 shows large NDVI interannual differences for the winter period associated to two pure FPH/DEC points in the same field plot (1 and 2 in
Figure 28A).Additionally, another factor potentially lowering classification accuracy is the absence of any pure pixel related to the FPH/EVR class (Evergreen).This is mainly due to the small number of currently available GHC field plot data. FPH/EVR is relatively abundant in Mediterranean habitats, thus their influence in classification is possibly not negligible.

2) Using reference data derived uniquely from spectral information with its own classification errors to calculate classification accuracy (JRC Forest Map 2006) can lead to misleading accuracy results and in this case a higher degree of 'mismatches' between the compared datasets. This is especially true when the background component is strong, and forest density low (such as in the MDN zone).
Figure 28*B* shows the overlap between the JRC Forest Map 2006 (darker green, broad-leaved) within the previous GHC FPH/DEC polygons. Mismatches between the two are evident (barycentres of MODIS pure pixels shown as red points). This highlights one important issue with continental or global scale EO derived products: there is a widespread lack of available high quality and independent data suitable for validation.

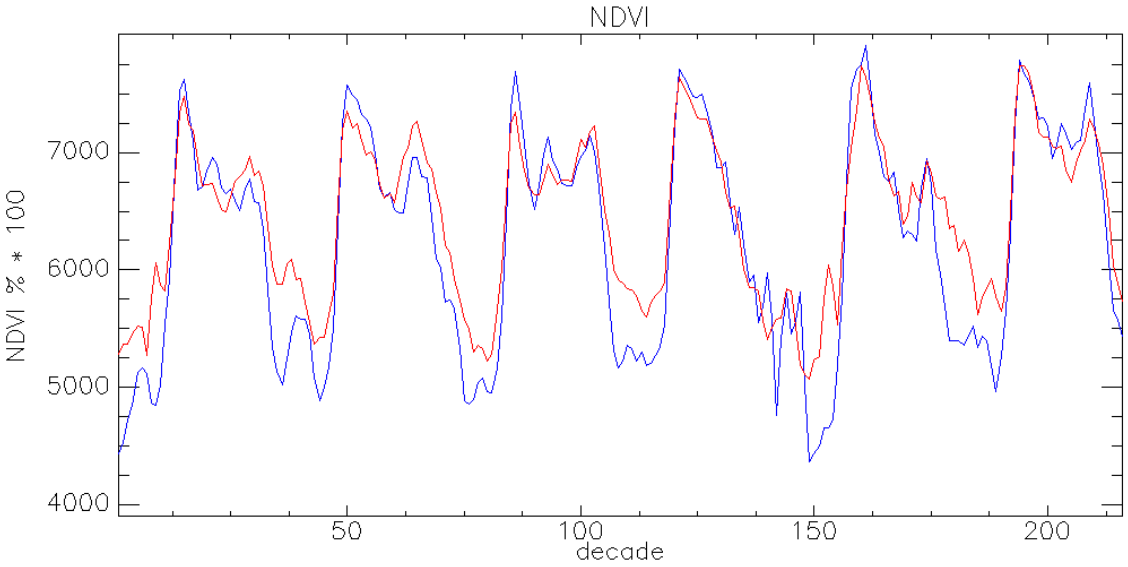

Figure 27. NDVI interannual run for two FPH/DECpure points in the same field plot (see next Figure in the upper part for locations of Point 1-red- and Point 2-blue-).

It is clear from the two classification tests in coniferous and deciduous dominated sites (Austria and MDN zone),how the classification accuracy depends largely on site specific conditions. Especially when the tree density is low revealing a large amount of background (e.g. under storey of shrubs, herbs, herbaceous, forbs or soil) is high in the forest stand, the inter-annual NDVI run can appear significantly different, hence influencing phenology indicators values. Selecting the best performing phenometrics did not lead to the expected accuracy improvement, appearing to be a secondary factor of importance with respect to the site specific forest characteristics.

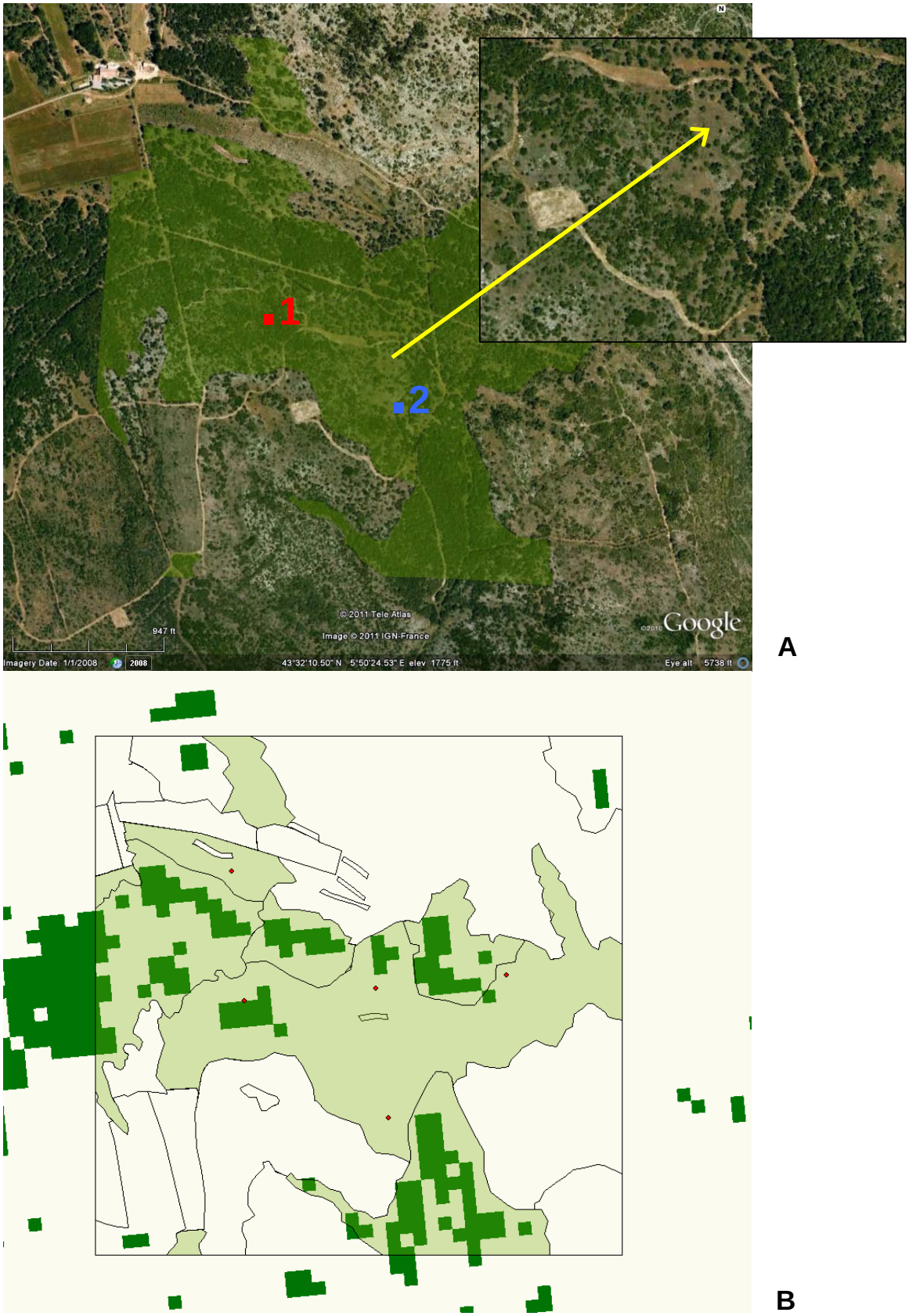

Figure 28. FPH/DEC polygons on (A)GoogleEarth® images and (B)on JRC Forest Mask 2006.

4.2.4 Influence of NDVI data gaps in Classification

Time series of vegetation indices are often characterized by the presence of data gaps. These are due to atmospheric events, like cloud coverage, snow and smoke which do not allow adequate detection of the vegetation spectral signal. Both number and sequential arrangement of these gaps can have an influence on the performance of a classification by altering the data quality. Here we assessed the potential impact these data gaps could have on the performance of phenology based GHC RF classifications.

A set of MODIS representing pure pixels of FPH/CON and FPH/DEC showing no data gaps (no interpolated values in the series of NDVI MVC decades) were selected. The 'purity' criterion is the same as applied in *Section 4.2.2*. All pixels were chosen with the condition of being located within the Mediterranean North zone –MDN- (Metzger et al., 2005), but also to have a correspondent pixel in the JRC Map 2006 validation dataset at 250 m. The spatial constraint was adopted to minimize the influence of bio-geographical variations in forest composition, focusing on regions with homogeneous bioclimatic conditions. The number of training points was limited to a total of 10.

The following processing steps were followed:

- Introduction of 10 consecutives 'data gaps' (10 contiguous data gaps decades) per year within the full 6 years MODIS NDVI time series;
- Extraction of the FPH/CON and FPH/DEC training (pure) pixels from the modified NDVI time series (series with data gaps added);
- RF Classifications using all the phenometrics for the NDVI time series with data gaps added;
- Accuracy assessment and comparison with classification accuracy using the original NDVI data.

Figure 29. Location of pure pixels (red) selected within the MDN Environmental Zone (light green).

Figure 30 shows the count of data gaps (i.e. no of decades available to build a seasonal mean) present within the MODIS NDVI time series after pre-processing operations (*Section 3.2*). Data gaps occur mainly in the Northern areas and in mountainous regions, and range between 0 and 25 in the European territory. To investigate their influence on GHCs classification accuracy, a series of data gaps were artificially introduced in the NDVI time series of FPH/CON and FPH/DEC pure pixels previously used to train the RF classifier.

The pre-processing chain applied to the NDVI data is partly able to cope with data gaps, especially if they are of short lengths. When seasonal means are available, the data gap is replaced by this value. When seasonal means cannot be calculated, data is linearly interpolated between the existing gap-contiguous data points. For longer data gaps this may imply serious problems, especially if significant vegetation dynamics are expected within the missing time gap. The impact is generally attenuated due the fact that gaps are occurring for the majority during winter time, when vegetation activity is low. But still, the majority of phenological indicators (e.g. minimum, start and end of season, etc.) rely on parameters extracted in this period.

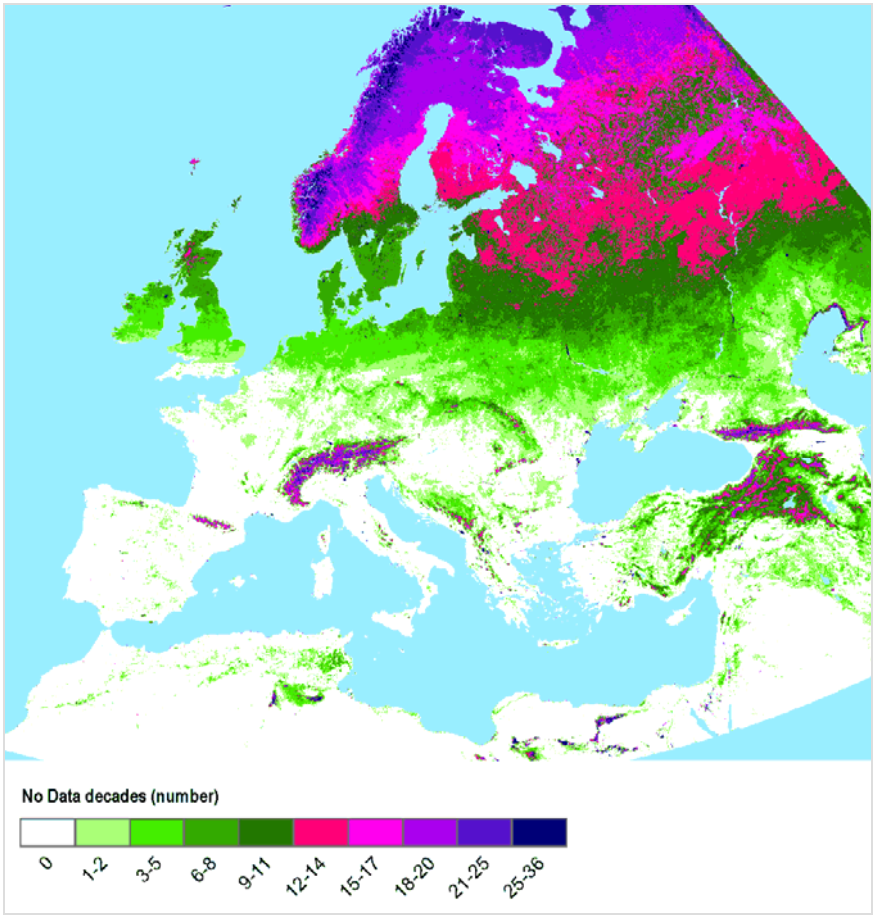

Figure 30. Count of no data decades in the MODIS NDVI time series after pre-processing operations.

Five pure pixel points from GHC field plots in South Sweden are shown to explore the effect of pre-processing on NDVI time series in regions largely affected by data gaps. The common number of missing decades for all 5 points is 8 decades for the winter 2004/2005 and 10, 10, 9 and 11 for the following winters. Smaller gaps outside the winter period do not exceed 3 decades. The gaps are generally located symmetrically around the turn of the year (*Figure 31A*). Missing data and outliers are substituted by seasonal means (*Figure 31B*). The outlier criterion was chosen according to Chebychev's theorem (95% confidence interval, see Lohninger, 1999). The '0' value visible around the turn of the year was used to identify missing data when using integer type. Finally (*Figure 31C*), missing data which could not be substituted with the seasonal mean are given an interpolated value using the nearest existing points in time and subsequently filtered using Savitzky-Golay algorithms (Chen et al., 2004).

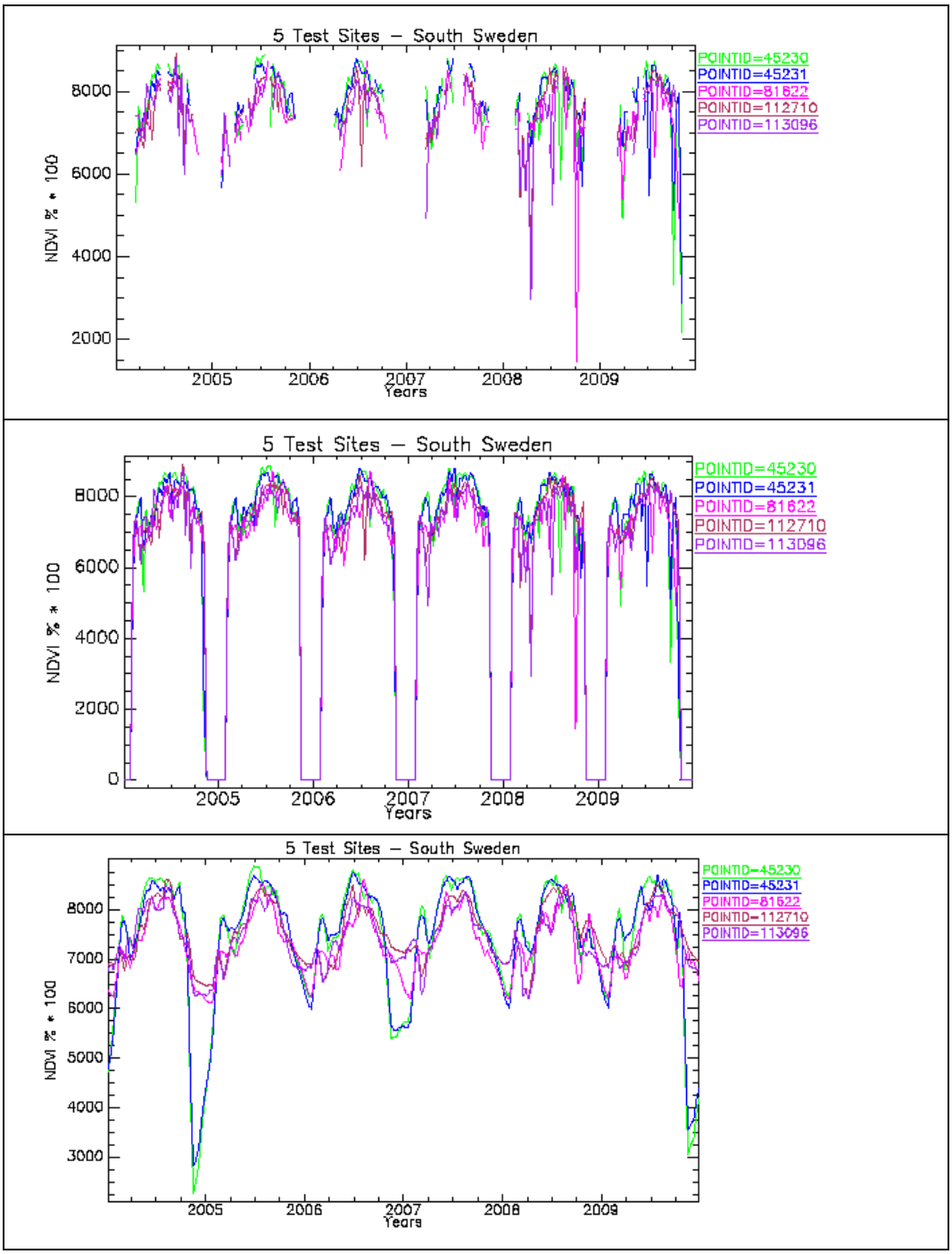

Figure 31. Time series of NDVI for five selected points for three pre-processing steps.

Filtering delivers a better representation of the real run of the vegetation cycle, attenuating or eliminating artefacts, as the ones visible in April and October 2008 in *Figure 31A*. However, some other artefacts (e.g. around November 2004) are not eliminated by the filter and recognized as valid data. Also, due to a missing reference, it is not clear which values would in reality correspond to proper winter minima for the presented vegetation cycles. In *Figure*

31C the lowest values calculated (excluding the drop in autumn 2004) assumes NDVIs on average around 0.6. As observed, the original NDVI data, in order to be adequately prepared for the extraction of phenometrics, are manipulated through a large number of processing steps that make use of a series of different assumptions and processing algorithms.

Statistics of single NDVI decades revealed that the majority of no data flags occur in winter period, January and December being the most affected months. This time interval was chosen as the more adequate to introduce the artificial no data sequences in order to simulate a real-like situation; the length of no data segments introduced is equal to 10 decades each. A comparison of the processing steps for a sample point for original NDVI time series and the same with added data gaps is shown in *Figure* 32 (A, original NDVI data series; B, substitution with seasonal means and outlier analysis; C, interpolate no data values between nearest existing points in time; D, Savitzky-Golay filtering).

After modification of the original NDVI series, the extraction of phenometrics using Phenolo was launched again for the MDN zone. The values of the phenology indicators for the CON and DEC training pixels were extracted.A RF classification is then launched using the same configuration as used for the data series with no gaps added (all phenometrics). An accuracy assessment, using the JRC Forest Map 2006, represented the final step. Results are reported in the following table, together with accuracy values of the classification with original NDVI data.

Table 14. Class and overall classification accuracy for the Ph0 phenometric configuration (31 phenometrics) using original NDVI values and with added data gaps.

Class Accuracy (%)	***Ph0 with data gaps added***	***Ph0 original Data***	***Accuracy Decrease***
Coniferous – CON	57.12%	57.40%	<1%
Deciduous – DEC	67.32%	67.63%	<1%
Overall Map Accuracy (%)	**77.24%**	**77.46%**	**<1%**

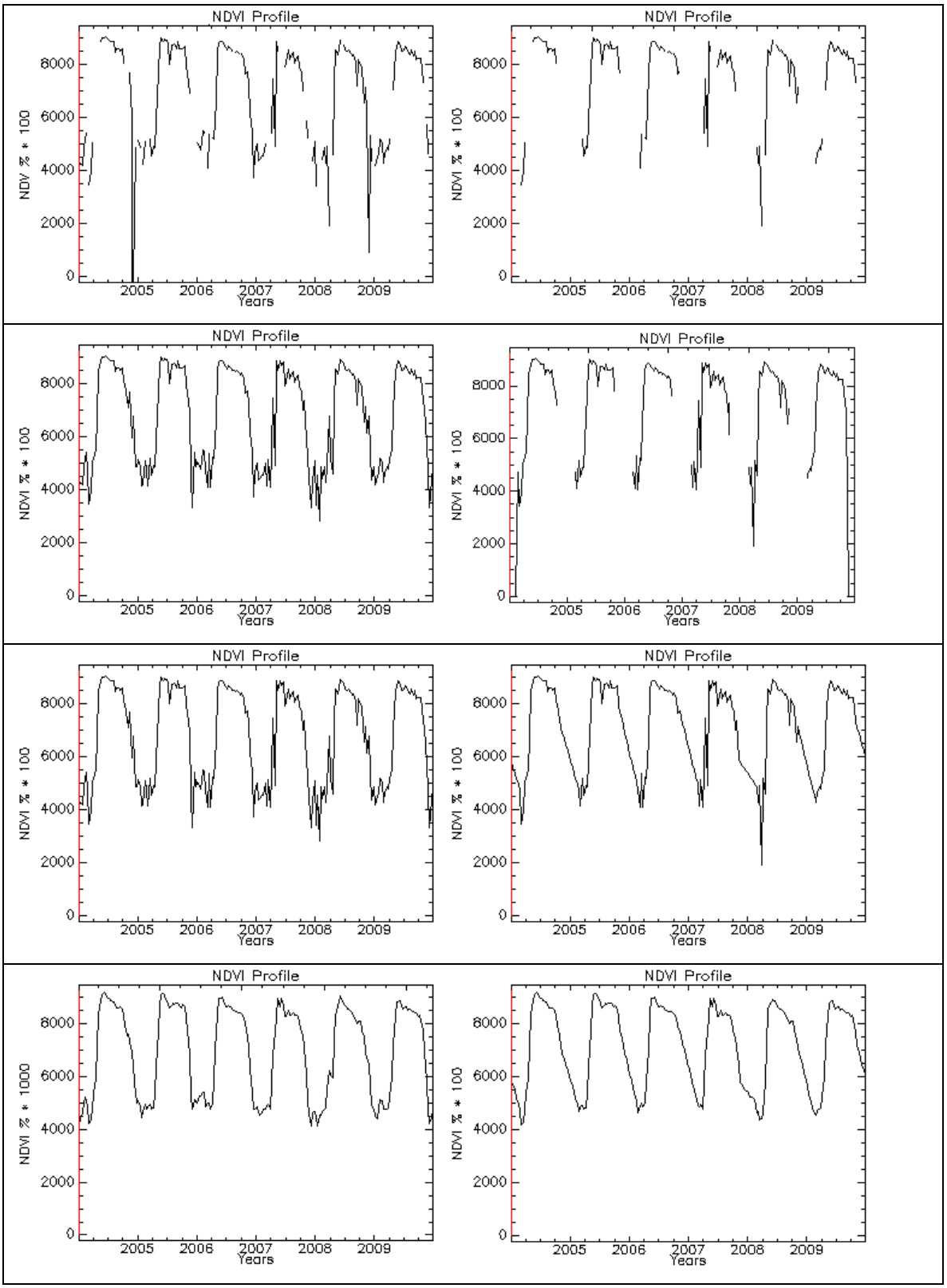

Figure 32. NDVI time series at different steps of the pre-processing chain for the original data (left column) and with added data gaps (right column); sample point of Deciduous forest.

Classification accuracies using NDVI data with and without added gaps differ less than 1%. Insertion of data gaps, contiguous and located in the same temporal windows, did not produced remarkable effects in the extraction of date and productivity phenometrics. Pre-processing operations dealt effectively with data gaps: substitution/filtering operations generally produced plausible continuous NDVI time series (e.g. *Figure* 32*D*). Due to time constraints it was not possible to test other data gaps configurations, like non continuous gaps, no data segments longer than 10 decades or with random distribution, etc. As a consequence, in order to infer general conclusions on data gaps influence on classification further tests are needed to cover a variety of data gaps distributions and applied to other regions (e.g. Boreal). Nevertheless, when the NDVI data series is characterized for a large part by data with few substituted values (as in the MDN zone) and data gaps are located in the NDVI time series minima, data gaps appear to influence classification accuracy less than the site specific characteristics of forest stands.

An analysis to test the statistical significance of change in phenometrics extracted from original data and from data with added gaps was performed using a random subset of 4,085 points. The majority of phenometrics show a statistically significant change (*Table 15*). Boxplots of paired phenometrics are illustrated in *Figure 33*.

Table 15. Significance levels (stating that samples means are statistically different) for paired t-test between phenometric data without and with gaps. Significance levels: n.s: not significant (or p-value >= 0.01), *: 0.005 < p <= 0.01, **: 0.001 < p <= 0.005, ***: p <= 0.001. Samples number = 4,085.

B1_sbd	***	B17_mbd	***
B2_sbv	***	B18_mbv	***
B3_sed	***	B19_med	***
B4_sev	***	B20_mev	***
B5_sl	***	B21_ml	***
B6_si	***	B22_mi	***
B7_sni	***	B23_mni	***
B8_str	***	B24_mtr	***
B9_spi	***	B25_mpi	***
B10_ged	***	B26_sei	n.s.
B11_gev	***	B27_gei	n.s.
B12_gl	n.s.	B28_sbc	n.s.
B13_gi	*	B29_ssd	***
B14_gni	***	B30_mxd	n.s.
B15_gtr	excluded	B31_mxv	***
B16_gpi	n.s.	B32_omi	***

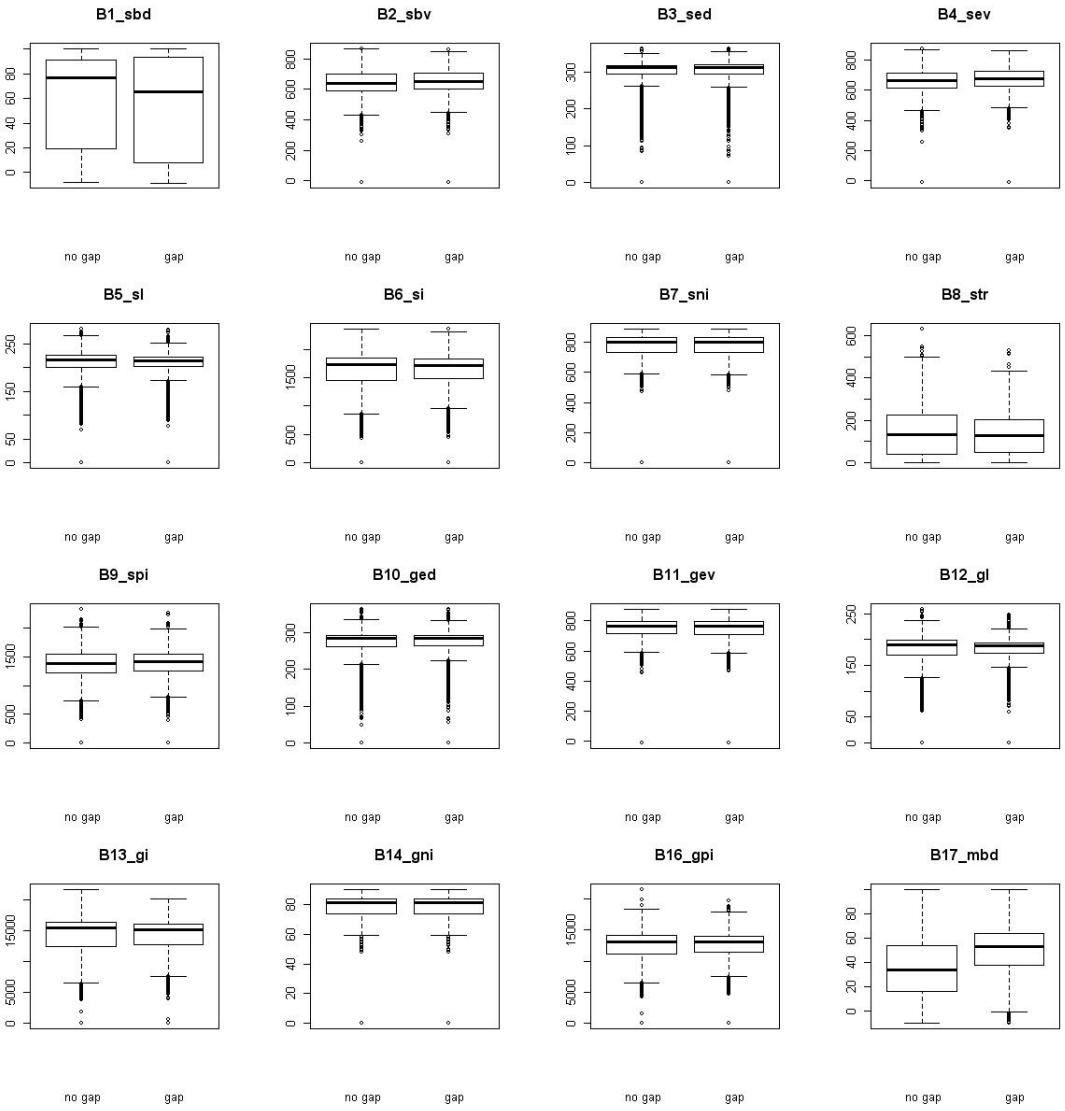

Figure 33. Boxplots of compared phenometrics values extracted by MODIS data of original and with no data gaps added (4,085 random points).

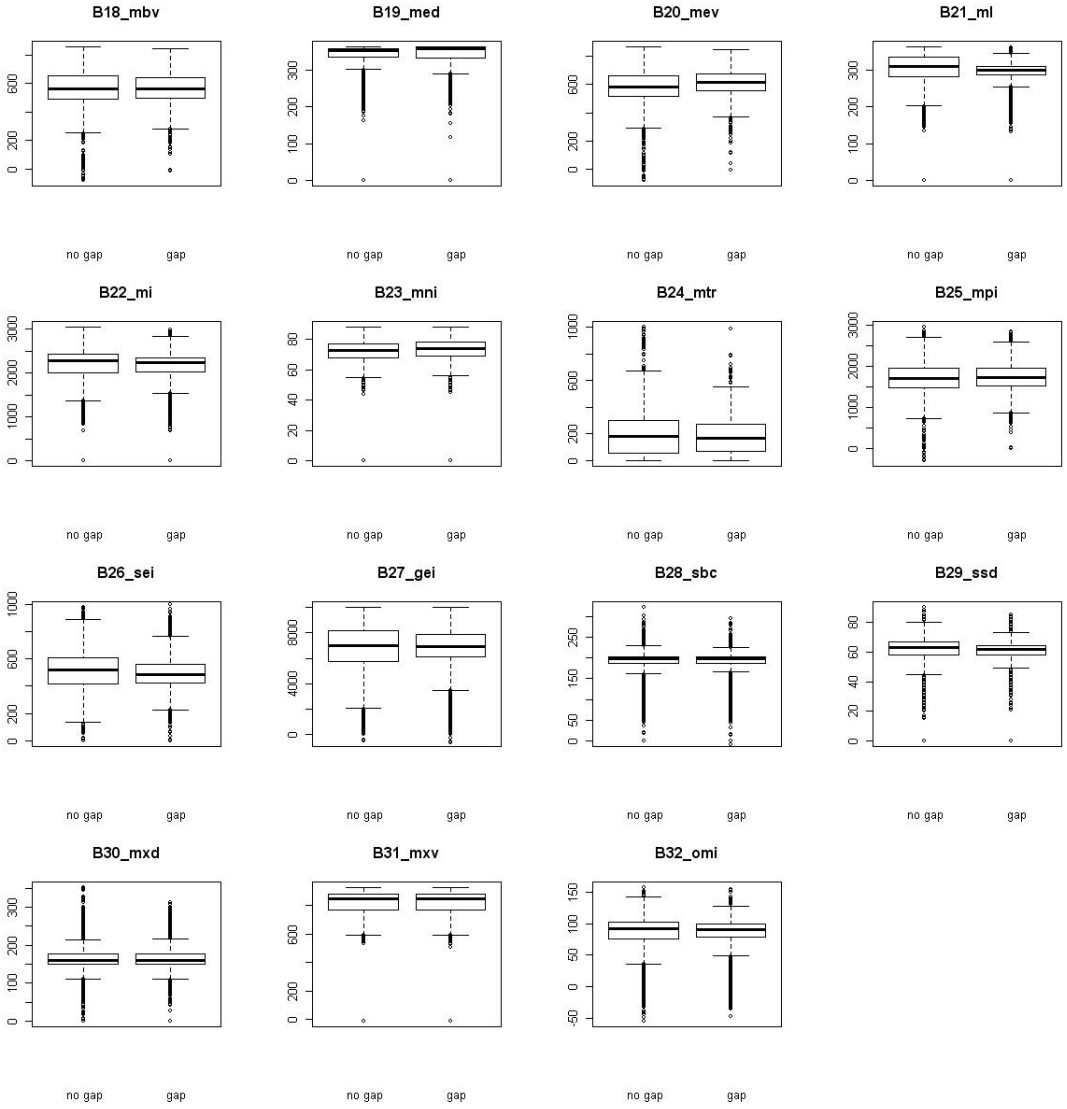

Figure 33 (continued). Boxplots of compared phenometrics values extracted by MODIS data of original and with no data gaps added (4,085 random points).

5. Conclusions and recommendations

The JRC Phenolo model (ver. 2009) allowed the extraction of a large set of date and productivity phenology indicators from SPOT and MODIS NDVI time series. Model coded in IDL provided fast calculations within a stable environment. The degree of information redundancy (based on calculations of correlation matrix) present among the 31 Phenolo phenometrics suggests it is possibly to focus on smaller sets of indicators instead than a large set of metrics without reducing the effectiveness of a classification.

We have demonstrated that the Random Forests classification technique is an attractive method for classifying remotely sensed data because of the following reasons: 1) it is very fast in training large datasets, 2) it provides an error measure based on the set of training pixels (OOB), and more importantly 3) the RF algorithm gives an indication of variables importance in the classification (Gislason et al., 2004). In the tests performed, the Mean Decrease Accuracy (MDA) calculation generally indicated *date phenometrics* as more important for classification than productivity phenometrics. The most recurrent phenology indicators (top of MDA graphs) were located around the Peak of Season point (MXV, MXD) and the curve absolute minima (MBV, MEV). Nevertheless, further analyses are needed to infer more general rules on single phenometrics importance, as defined by Phenolo, for habitat classification. The OOB error did not show a recurrent pattern. In our tests, in presence of correlated phenometrics and well differentiated training pixels among classes, the use of a small selected set of phenology indicators produced higher classification accuracy. This trend can be different when these conditions are not respected, such as using noisy training datasets.

Apart from spatially and spectrally homogeneous classes (FPH/CON in Austria), the overall classification accuracy achieved based on Random Forests and MODIS-based phenology indicators is generally not satisfactory. The following factors were considered to negatively influence the intercalibration exercise:
1) The spatial heterogeneity present in the GHC forest polygons delineated in the field work is potentially a high influencing factor. This heterogeneity produces remarkable variance associated with the NDVI trends of training pixels, and consequently in the values of the phenology indicators entering the classification. The GHC system in fact makes use of *general* categories, which can be very heterogeneous in the same class, thus producing also heterogeneous signals at spectral level. Our analysis indicated this is particularly evident in vegetation stands with large soil component and sparse trees clumping.

2) The number of GHC field plots data currently available did not allow to retrieve a large set of pure pixels to train the RF classifier. Also, no pure pixels were obtainable for the FPH/EVR class. To take into account the high variability of forest stand characteristics in European environments a large set of training points it is necessary as input to the classification.
3) The accuracy assessment was performed using the JRC Forest Map 2006. As this dataset is built uniquely on spectral information an assessment of accuracy can lead to increased 'mismatches' between the compared GHC data (whose classes are not defined on a spectral basis) and the JRC Forest Map 2006.

The introduction of artificial data gaps within the MODIS NDVI time series was not very relevant towards classification accuracy (test for the MDN environmental zone). The applied pre-processing operations effectively dealt with no data decades by reconstructing reasonable NDVI curves. Changes in artificial gaps configuration (number, time location, etc) and zone of analysis could potentially provide more noise in the signal, and affect more significantly the classification accuracy.

On the basis of the above results our concluding remarks are as follows:

- The spatial scale of current EO-based phenology data (250 m) is at the edge of an adequate resolution for effective habitat classification with respect to the GHC categories. MODIS 250 m grid overlapped on high resolution GHC field plots provide polygons with a variety of mixed classes, which are difficult to classify and unmix.
- For the intercalibration of GHCs with EO-based phenology indicators, the production and use of a large dataset of GHC training pixels ('pure pixels') is recommended to take into account the high spectral variability present within single GHC classes. This can be achieved by the sampling of several field plots in different Environmental Zones with a variety of local conditions.
- An adequate classification accuracy assessment should be based on a reference dataset which is not processed uniquely on spectral information, but that is built taking into account as much as possible the elements of heterogeneity typical of the General Habitat Categories. This can be possibly addressed using regional or national habitat map and datasets.

To conclude, the elements (e.g. height of stand) characteristics of the life forms types considered in the General Habitat Category scheme are very valuable information to be taken into account in intercalibration using EO-derived information. For this reason and for the purpose of GHCs classification we believe that a strategy which integrates EO-based phenology indicators with other remotely sensed information, such as typically LiDAR or high resolution radar, can be potentially more effective than a purely phenology-based approach.

Acknowledgements

The authors thank Dr S.Kay and the MARS Unit of the EC JRC for providing the raw NDVI SPOT/MODIS data, Dr E.Ivits and team (EC JRC) for providing Phenolo software/material and Dr S.Mucher (Alterra, NL) for supplying the modelled habitat data for Austria and Slovakia. Thanks are due also to Dr F.Gerard (CEH) for insightful discussions and document revision, and Dr P.Zuccolotto, Dr M.Sandri (Univ.Brescia) for their suggestions with the Random Forests algorithms.

References

Breiman, L., J. H. Friedman, R. A. Olshen, and C. J. Stone. 1984. Classification and regression trees. Monterey, Calif., U.S.A.: Wadsworth, Inc.

Breiman, L., 2001. Random forests. *Machine Learning*, 45, 5-32. Elsevier.

Bunce R.G.H., Bogers, M.M.B., Evans, D and Jongman R.H.G. 2010. *D4.2: Rule based system for Annex I habitats.* EBONEDeliverable report. http://www.ebone.wur.nl/NR/rdonlyres/DADAAB1E-F07C-4AA3-8621-20548A9B7DE6/106197/EBONED42KeyAnnex1.pdf

Bunce, R.H.G., M.J. Metzger, R.H.G. Jongman, J. Brandt, G. de Blust, R. Elena Rossello, G. B. Groom, L. Halada, G. Hofer, D.C. Howard, P. Kovář, C. A. Mücher, E. Padoa-Schioppa, D. Paelinx, A. Palo, M. Perez-Soba, I. L. Ramos, P. Roche, H. Skånes, T. Wrbka, 2008. A Standardized Procedure for Surveillance and Monitoring European Habitats and provision of spatial data. *Landscape Ecology*, 23:11-25.

Bunce R.G.H., C.J. Barr, R.T. Clarke, D.C. Howard and A.M.J. Lane 1996. Land Classification for Strategic Ecological Survey. *J. of Environmental Management* 47:37-60.

Chen J., Jönsson P. , Tamura M., Gu Z., matsushita B., Eklundh L., *2004.* A simple method for reconstructing a high-quality NDVI time-series data set based on the Savitzky–Golay filter, *Remote Sensing of the Environment*91 , pp. 332–344.

EEA -European Environment Agency-, 2010. Corine Land Cover 2000 seamless vector data (Publish date: 27 May 2010).URL: http://www.eea.europa.eu/data-and-maps/data/corine-land-cover-2000-clc2000-seamless-vector-database-2

Geerken, R., Zaitchik B., Evans, J.P. 2005. Classifying rangeland vegetation type and fractional cover of semi-arid and arid vegetation covers from NDVI time-series, *International Journal of Remote Sensing*26(24), pp. 5535–5554.

Geerken, R., 2009. An algorithm to classify and monitor seasonal variations in vegetation phenologies and their inter-annual change. *ISPRS Journal of Photogrammetry and Remote Sensing*, Volume 64, Issue 4, July 2009, Pages 422-431.

Gislason, P.O, Benediktsson, J.A., Sveinsson, J.R., 2004. Random Forests for land cover classification, *Pattern Recognition Letters*, Volume 27, Issue 4, Elsevier.

Hill M. J., Donald, G.E., 2003. Estimating spatio-temporal patterns of agricultural pro-ductivity in fragmented landscapes using AVHRR NDVI time series. *Remote Sensing of Environment*, 84(3): 367-384

Hill, R.A., Granica, K., Smith, G. M. and Schardt, M., 2007. Representation of an Alpine Treeline Ecotone in SPOT HRG Data. *Remote Sensing of Environment*, 110 (4), pp. 458-467.

Holben, B.N., 1986. Characteristics of maximum-value composite images from temporal AVHRR data. *International Journal of Remote Sensing*, 7(11):1417-1437, pp. 562-571.

Ivits, E., M. Cherlet, W. Mehl, S. Sommer , 2008. Spatial Assesment of the Status of Riparian Zones and Related Effectiveness of Agri-Environmental Schemes in Andalusia, Spain , EUR Report, EUR 23299 N1018-5593, 80p, JRC Report, Luxembourg.

Ivits, E. Michael Cherlet, Wolfgang Mehl, Stefan Sommer, 2009. Estimating the ecological status and change of riparian zones in Andalusia assessed by multi-temporal AVHHR datasets,. *Ecological Indicators*, Volume 9, Issue 3, May 2009, Pages 422-431, DOI: 10.1016/j.ecolind.2008.05.013.

Jönsson, P., Eklundh, L., 2002. Seasonality extraction by function-fitting to time series of satellite sensor data. IEEE Transactions on Geoscience and Remote Sensing, 40, 1824−1832.

Jönsson, P., Eklundh, L., 2004. TIMESAT - a program for analysing time-series of satellite sensor data, *Computers and Geosciences* 30, 833-845.

Klisch, A. ,Royer, A.,Lazar C., Baruth, B., Genovese, G., 2005. Extraction of phenological parameters from temporally smoothed vegetation indices; ISPRS Archives XXXVI-8/W48 Workshop proceedings: Remote sensing support to crop yield forecast and area estimates.

Kempeneers, P., Sedano, F., Seebach, L., San Miguel Ayanz, J., 2010. A high resolution PAN-European forest type map based on multispectral and multi-temporal remote sensing data. Proceedings of ForestSat2010 Conference: Operational Tools in Forestry using Remote Sensing Techniques. 7-10 Semptember 2010, Lugo y Santiago de Compostela, Spain.

Koeble R., Seufert G., 2001. Novel Maps for Forest Tree Species in Europe. http://afoludata.jrc.ec.europa.eu/index.php/public_area/tree_species_distribution

Liaw, A., Wiener, M., 2002. Classification and Regression by RandomForests. R News 2(3), 18-22.

Liaw, A., Wiener, M. RandomForest: Breiman and Cutler's RandomForests for Classification and Regression, 2009. URL: http://cran.r-project.org/package=randomForest. R package version 4.5-30.

Lohninger, H., 1999.*Teach*/*Me Data Analysis*, Springer-Verlag, Berlin-New York-Tokyo.

Metzger, M. J., R. G. H. Bunce, et al. ,2005. A climatic stratification of the environment of Europe. *Global Ecology & Biogeography*. 14: 549-563.

Mücher, C.A., Hennekens, S.M., Bunce, R.G.H., Schaminée, J.H.J., Schaepman, M.E.
Modelling the spatial distribution of Natura 2000 habitats across Europe. 2009. *Landscape and Urban Planning*, 92 (2), pp. 148-159.

Paola, J. D., and Schowengerdt, R. A. 1995. A Review and Analysis of Backpropagation Neural Networks for Classification of Remotely Sensed Multispectral Imagery. *International Journal of Remote Sensing*, vol. 16, no. 16, pp. 3033-3058, November 10, 1995.

Pekkarinen, A., Reithmaier, L. & Strobl, P. 2009. Pan-European forest/non-forest mapping with Landsat ETM+ and CORINE Land Cover 2000 data. *ISPRS Journal of Photogrammetry and Remote Sensing* 64: 171-183.

Rahman, H. and G. Dedieu, 1994: SMAC: A simplified method for the atmospheric of satellite measurements in the solar spectrum. *International Journal of Remote Sensing*, 15, 123-143

Reed B C, Brown J.F., VanderZee D., Loveland,T.R., Merchant J.W., Ohlen, D.O. 1994. Measuring phenological variability from satellite imagery. *Journal of Vegetation Science*, 5(5): 703-714

Steenkamp K. Wessels K.J., Archibald S.A., Von Maltitz G. 2008. Long-term phenology and variability of Southern African vegetation. *IEEE International GeoSciences and Remote Sensing Society (IGARSS)* Symposium. Boston, Massachusetts, U.S.A., 6-11 July 2008.

Steinberg, D., Colla, P., 1995. CART: Tree-structured non-parametric data analysis. San Diego, Calif., U.S.A.: Salford Systems.

Weissteiner, C., Sommer, S., Strobl, P. 2007. Time series analysis of NOAA AVHRR Green vegetation fraction as a means to derive permanent and seasonal vegetation component.Proceedings from the EARSeL Workshops in the framework of the 27th Symposium. June 7-9, 2007. Bozen (Italy).

Wessels, K., Steenkamp, K., Von Maltitz, G., Archibald, S. 2011. Remotely sensed vegetation phenology for describing and predicting the biomes of South Africa. *Applied Vegetation Science* 14:49–66. Wiley.

Annex 1

Table A1. Pearson's correlation matrix among Phenolo indicators extracted from the MODIS NDVI data for Europe (395,584,800 points). In grey are highlighted correlations greater or equal than 0.9.

	SBD	SBV	SED	SEV	SL	SI	SNI	SPI	STR	GED	GEV	GL	GI	GNI	GPI	MBD	MBV	MED	MEV	ML	MI	MNI	MTR	MPI	SEI	GEI	SBC	SSD	MXD	MXV	OMI
SBD	1	0.19	0.77	0.26	-0.15	0.21	0.26	-0.02	0.18	0.82	0.24	-0.10	0.20	0.26	0.17	0.82	0.18	0.60	0.31	-0.35	0.18	0.28	-0.06	0.18	0.08	0.12	0.93	-0.33	0.84	0.26	-0.15
SBV	0.19	1	0.41	0.99	0.39	0.89	0.94	-0.22	0.95	0.41	0.97	0.42	0.88	0.93	0.93	0.07	0.97	0.36	0.96	0.23	0.92	0.97	-0.21	0.95	0.82	0.87	0.29	0.17	0.23	0.88	0.39
SED	0.77	0.41	1	0.49	0.51	0.60	0.52	0.02	0.54	0.96	0.50	0.49	0.58	0.52	0.53	0.50	0.32	0.84	0.46	0.18	0.54	0.52	0.01	0.43	0.31	0.41	0.90	0.18	0.76	0.53	0.51
SEV	0.26	0.99	0.49	1	0.41	0.91	0.96	-0.21	0.96	0.48	0.97	0.43	0.90	0.95	0.93	0.13	0.95	0.43	0.97	0.23	0.93	0.98	-0.20	0.95	0.81	0.87	0.37	0.18	0.28	0.90	0.41
SL	-0.15	0.39	0.51	0.41	1	0.65	0.45	0.06	0.59	0.39	0.46	0.90	0.63	0.46	0.61	-0.32	0.26	0.50	0.29	0.75	0.60	0.44	0.11	0.44	0.38	0.47	0.14	0.74	0.06	0.47	1.00
SI	0.21	0.89	0.60	0.91	0.65	1	0.96	-0.08	0.96	0.56	0.96	0.66	0.99	0.95	0.97	0.00	0.78	0.56	0.81	0.47	0.98	0.95	-0.08	0.86	0.77	0.84	0.39	0.37	0.28	0.94	0.65
SNI	0.26	0.94	0.52	0.96	0.45	0.96	1	-0.10	0.92	0.51	0.99	0.49	0.95	1.00	0.93	0.09	0.86	0.48	0.88	0.31	0.95	0.99	-0.12	0.87	0.78	0.84	0.38	0.19	0.28	0.99	0.45
SPI	-0.02	-0.22	0.02	-0.21	0.06	-0.08	-0.10	1	-0.19	0.01	-0.13	0.05	-0.07	-0.09	-0.14	-0.06	-0.27	0.05	-0.25	0.10	-0.11	-0.14	0.23	-0.23	-0.17	-0.17	-0.01	0.03	-0.02	-0.05	0.06
STR	0.18	0.95	0.54	0.96	0.59	0.96	0.92	-0.19	1	0.51	0.94	0.60	0.94	0.91	0.98	0.02	0.89	0.49	0.90	0.39	0.96	0.94	-0.16	0.95	0.81	0.88	0.35	0.36	0.26	0.87	0.59
GED	0.82	0.41	0.96	0.48	0.39	0.56	0.51	0.01	0.51	1	0.50	0.49	0.58	0.51	0.54	0.54	0.33	0.78	0.45	0.09	0.51	0.51	0.00	0.42	0.31	0.35	0.92	0.10	0.82	0.51	0.39
GEV	0.24	0.97	0.50	0.97	0.46	0.96	0.99	-0.13	0.94	0.50	1	0.50	0.95	0.99	0.95	0.07	0.89	0.46	0.90	0.32	0.96	0.99	-0.14	0.90	0.81	0.86	0.36	0.21	0.27	0.97	0.46
GL	-0.10	0.42	0.49	0.43	0.90	0.66	0.49	0.05	0.60	0.49	0.50	1	0.69	0.48	0.67	-0.30	0.29	0.43	0.31	0.68	0.62	0.47	0.10	0.46	0.42	0.43	0.18	0.68	0.15	0.48	0.90
GI	0.20	0.88	0.58	0.90	0.63	0.99	0.95	-0.07	0.94	0.58	0.95	0.69	1	0.95	0.98	-0.01	0.76	0.55	0.79	0.47	0.97	0.93	-0.07	0.84	0.76	0.81	0.38	0.37	0.28	0.94	0.63
GNI	0.26	0.93	0.52	0.95	0.46	0.95	1.00	-0.09	0.91	0.51	0.99	0.48	0.95	1	0.92	0.09	0.84	0.49	0.86	0.31	0.95	0.99	-0.11	0.86	0.77	0.83	0.38	0.18	0.27	0.99	0.45
GPI	0.17	0.93	0.53	0.93	0.61	0.97	0.93	-0.14	0.98	0.54	0.95	0.67	0.98	0.92	1	-0.03	0.84	0.48	0.85	0.43	0.97	0.94	-0.13	0.91	0.80	0.84	0.34	0.38	0.27	0.89	0.60
MBD	0.82	0.07	0.50	0.13	-0.32	0.00	0.09	-0.06	0.02	0.54	0.07	-0.30	-0.01	0.09	-0.03	1	0.10	0.46	0.22	-0.66	-0.06	0.13	-0.09	0.00	-0.20	-0.13	0.73	-0.54	0.66	0.07	-0.32
MBV	0.18	0.97	0.32	0.95	0.26	0.78	0.86	-0.27	0.89	0.33	0.89	0.29	0.76	0.84	0.84	0.10	1	0.27	0.97	0.12	0.83	0.91	-0.27	0.95	0.80	0.83	0.25	0.06	0.20	0.78	0.26
MED	0.60	0.36	0.84	0.43	0.50	0.56	0.48	0.05	0.49	0.78	0.46	0.43	0.55	0.49	0.48	0.46	0	1	0.39	0.36	0.53	0.47	0.03	0.42	0.37	0.45	0.78	0.33	0.65	0.50	0.50
MEV	0.31	0.96	0.46	0.97	0.29	0.81	0.88	-0.25	0.90	0.45	0.90	0.31	0.79	0.86	0.85	0.22	0.97	0.39	1	0.10	0.84	0.93	-0.25	0.95	0.78	0.83	0.37	0.07	0.30	0.81	0.29
ML	-0.35	0.23	0.18	0.23	0.75	0.47	0.31	0.10	0.39	0.09	0.32	0.68	0.47	0.31	0.43	-0.66	0.12	0.36	0.10	1	0.51	0.26	0.12	0.35	0.53	0.52	-0.11	0.84	-0.15	0.34	0.75
MI	0.18	0.92	0.54	0.93	0.60	0.98	0.95	-0.11	0.96	0.51	0.96	0.62	0.97	0.95	0.97	-0.06	0.83	0.53	0.84	0.51	1	0.95	-0.11	0.92	0.88	0.93	0.35	0.40	0.25	0.93	0.59
MNI	0.28	0.97	0.52	0.98	0.44	0.95	0.99	-0.14	0.94	0.51	0.99	0.47	0.93	0.99	0.94	0.13	0.91	0.47	0.93	0.26	0.95	1	-0.16	0.91	0.79	0.85	0.39	0.18	0.29	0.96	0.44
MTR	-0.06	-0.21	0.01	-0.20	0.11	-0.08	-0.12	0.23	-0.16	0.00	-0.14	0.10	-0.07	-0.11	-0.13	-0.09	-0.27	0.03	-0.25	0.12	-0.11	-0.16	1	-0.23	-0.17	-0.17	-0.03	0.11	-0.03	-0.08	0.11
MPI	0.18	0.95	0.43	0.95	0.44	0.86	0.87	-0.23	0.95	0.42	0.90	0.46	0.84	0.86	0.91	0.00	0.95	0.42	0.95	0.35	0.92	0.91	-0.23	1	0.90	0.94	0.30	0.28	0.23	0.80	0.44
SEI	0.08	0.82	0.31	0.81	0.38	0.77	0.78	-0.17	0.81	0.31	0.81	0.42	0.76	0.77	0.80	-0.20	0.80	0.37	0.78	0.53	0.88	0.79	-0.17	0.90	1	0.96	0.20	0.39	0.15	0.74	0.38
GEI	0.12	0.87	0.41	0.87	0.47	0.84	0.84	-0.17	0.88	0.35	0.86	0.43	0.81	0.83	0.84	-0.13	0.83	0.45	0.83	0.52	0.93	0.85	-0.17	0.94	0.96	1	0.25	0.40	0.17	0.80	0.47
SBC	0.93	0.29	0.90	0.37	0.14	0.39	0.38	-0.01	0.35	0.92	0.36	0.18	0.38	0.38	0.34	0.73	0.25	0.78	0.37	-0.11	0.35	0.39	-0.03	0.30	0.20	0.25	1	-0.08	0.85	0.37	0.14
SSD	-0.33	0.17	0.18	0.18	0.74	0.37	0.19	0.03	0.36	0.10	0.21	0.68	0.37	0.18	0.38	-0.54	0.06	0.33	0.07	0.84	0.40	0.18	0.11	0.28	0.39	0.40	-0.08	1	-0.13	0.18	0.74
MXD	0.84	0.23	0.76	0.28	0.06	0.28	0.28	-0.02	0.26	0.82	0.27	0.15	0.28	0.27	0.27	0.66	0.20	0.65	0.30	-0.15	0.25	0.29	-0.03	0.23	0.15	0.17	0.85	-0.13	1	0.28	0.05
MXV	0.26	0.88	0.53	0.90	0.47	0.94	0.99	-0.05	0.87	0.51	0.97	0.48	0.94	0.99	0.89	0.07	0.78	0.50	0.81	0.34	0.93	0.96	-0.08	0.80	0.74	0.80	0.37	0.18	0.28	1	0.47
OMI	-0.15	0.39	0.51	0.41	1.00	0.65	0.45	0.06	0.59	0.39	0.46	0.90	0.63	0.45	0.60	-0.32	0.26	0.50	0.29	0.75	0.59	0.44	0.11	0.44	0.38	0.47	0.14	0.74	0.05	0.47	1


ALTERRA
WAGENINGEN UR
CEH
Centre for Ecology & Hydrology
NATURAL ENVIRONMENT RESEARCH COUNCIL
THE UNIVERSITY OF EDINBURGH
CSIR
our future through science
SLU
Sveriges lantbruksuniversitet
ile
SAS
Institute of Landscape Ecology Slovak Academy of Sciences
HELMHOLTZ CENTRE FOR ENVIRONMENTAL RESEARCH – UFZ
NINA
Cemagref
UNIVERSIDAD POLITECNICA MADRID
רשות הטבע והגנים
inbo
Facultatea de Biologie
Universitatea din Bucureşti
umweltbundesamt
JRC
EUROPEAN COMMISSION
universität wien
Eesti Maaülikool
EMU
Estonian University of Life Sciences
ARISTOTLE UNIVERSITY OF THESSALONIKI